PLOS PATHOGENS

RESEARCH ARTICLE

High-risk human papillomavirus oncogenes disrupt the Fanconi anemia DNA repair pathway by impairing localization and de-ubiquitination of FancD2

Sujita Khanal, Denise A. Galloway*

Division of Human Biology, Fred Hutchinson Cancer Research Center, Seattle, Washington, United States of America

* dgallowa@fhcrc.org

Citation: Khanal S, Galloway DA (2019) High-risk human papillomavirus oncogenes disrupt the Fanconi anemia DNA repair pathway by impairing localization and de-ubiquitination of FancD2. PLoS Pathog 15(2): e1007442. https://doi.org/10.1371/journal.ppat.1007442

Editor: Robert F. Kalejta, University of Wisconsin-Madison, UNITED STATES

Received: October 25, 2018

Accepted: February 4, 2019

Published: February 28, 2019

Data Availability Statement: All relevant data are within the manuscript and its Supporting Information files.

Funding: This work was supported by R01 CA064795 (DAG) and R35 CA209979 (DAG). The funders had no role in study design, data collection and analysis, decision to publish, or preparation of the manuscript.

Competing interests: The authors have declared that no competing interests exist.

Abstract

Persistent expression of high-risk HPV oncogenes is necessary for the development of anogenital and oropharyngeal cancers. Here, we show that E6/E7 expressing cells are hypersensitive to DNA crosslinking agent cisplatin and have defects in repairing DNA interstrand crosslinks (ICL). Importantly, we elucidate how E6/E7 attenuate the Fanconi anemia (FA) DNA crosslink repair pathway. Though E6/E7 activated the pathway by increasing FancD2 monoubiquitination and foci formation, they inhibited the completion of the repair by multiple mechanisms. E6/E7 impaired FancD2 colocalization with double-strand breaks (DSB), which subsequently hindered the recruitment of the downstream protein Rad51 to DSB in E6 cells. Further, E6 expression caused delayed FancD2 de-ubiquitination, an important process for effective ICL repair. Delayed FancD2 de-ubiquitination was associated with the increased chromatin retention of FancD2 hindering USP1 de-ubiquitinating activity, and persistently activated ATR/CHK-1/pS565 FancI signaling. E6 mediated p53 degradation did not hamper the cell cycle specific process of FancD2 modifications but abrogated repair by disrupting FancD2 de-ubiquitination. Further, E6 reduced the expression and foci formation of Palb2, which is a repair protein downstream of FancD2. These findings uncover unique mechanisms by which HPV oncogenes contribute to genomic instability and the response to cisplatin therapies.

Author summary

High-risk human papillomavirus (HPV) causes nearly all cervical and many other anogenital cancers, and oropharyngeal cancers. As cisplatin is the most commonly used drug for cervical and HPV-associated oropharyngeal cancers, it is important to understand how HPV oncogenes disrupt the Fanconi anemia (FA) pathway involved primarily in the repair of cisplatin-induced DNA crosslinks. However, the mechanism by which HPV E6 and E7 attenuate the FA pathway is poorly understood. We demonstrate that E6/E7 expression disrupts crosslink repair and increase cisplatin sensitivity, and attenuate the

FA pathway through multiple unique mechanisms. First, E6/E7 causes accumulation of FancD2, a central component of the FA pathway, at the sites away from DNA damage. This results in reduced recruitment of Rad51, another repair protein involved in the pathway. Second, E6 causes delayed FancD2 de-ubiquitination, an important process for effective repair. Third, E6 expressing cells decreases the expression and foci formation of Palb2 repair protein. Together, this work elucidates the mechanisms by which HPV attenuates the repair of DNA crosslinks increasing cisplatin cytotoxicity and efficacy in treating HPV-positive cancers.

Introduction

High-risk human papillomavirus (HR-HPV) E6/E7 oncoproteins are essential for the development of malignancies of the anogenital tract and oropharynx, with HPV16 being the predominant type [1]. Cervical and oropharyngeal cancers are the most common HPV-associated malignancies among females and males, respectively [2]. Persistent HPV infection destabilizes the cellular genome which can lead to cancer. Genomic instability is likely the result of the numerous interactions of HPV oncoproteins with host tumor suppressors and DNA damage repair (DDR) proteins. Recently, we demonstrated that high-risk HPV oncogenes attenuate double-strand break (DSB) repair by impairing the homologous recombination pathway [3]. To further elucidate the mechanisms by which HPV oncogenes impair DDR, the present study focuses on the impact of HPV16 oncogenes on the Fanconi anemia-BRCA (FA or FA-BRCA) pathway.

The FA-BRCA pathway is involved in the repair of intra or interstrand crosslinks (ICL), thereby maintaining genomic stability [4, 5] (S1 Fig). ICLs block DNA replication and transcription and, thus, are highly cytotoxic to cells if not repaired. The FA pathway is composed of 22 FA proteins (identified to date) [6]. When any one of the FA genes of the FA-BRCA pathway is mutated, individuals have a spectrum of disorders, called Fanconi Anemia, characterized by bone marrow failure, congenital malformations, cancer predisposition, and cellular sensitivity to ICL-inducing agents [7]. Upon exposure to DNA crosslinking agents, and during S-phase of the cell cycle, ATR/CHK1 signaling gets activated and helps in the formation of an ubiquitin ligase complex (FA core complex), which is composed of eight FA proteins (FancA, -B, -C, -E, -F, -G, -L, and -M) with other associated proteins (such as FAAP-24, MHF2). Among the FA core complex subunits, FancM recognizes the stalled replication fork at the ICL site and forms a landing platform for the core complex [8]. Activated ATR/CHK1 phosphorylates several FA proteins including FancM, FancD2, and FancI [9]. The FA core complex through its E3 ubiquitin ligase subunit FANCL and the corresponding E2 ubiquitin-conjugating enzyme (UBE2T/ FancT) catalyzes the monoubiquitination of the FancD2-FancI heterodimer. Monoubiquitinated FancD2 (FancD2-Ub) and FancI-Ub form discrete nuclear foci at double-strand breaks (DSB) created at ICL-stalled replication forks, and subsequently recruit downstream DNA repair proteins, including FancD1 (BRCA2), FancS (BRCA1), FancR (Rad51), FancN (Palb2), and FancJ (BRIP1). These proteins in nuclear foci co-operate with other DNA repair pathways such as nucleotide excision repair, homology recombination, and translesion synthesis to repair ICLs [8]. Once DNA is repaired, the FA pathway is turned off by de-ubiquitination of the FancD2/ FancI complex to prevent prolonged cell cycle arrest and cell death [10]. FancD2/ FancI de-ubiquitination is catalyzed by the ubiquitin-specific protease USP1, in conjunction with UAF1 (USP1-associated factor 1). While monoubiquitination of FancD2 is essential for ICL repair, its deubiquitination by the USP1-UAF1 complex is also

critical for a functional FA pathway [10–14]. Knockout of either USP1 or UAF1 in mice causes an FA-like phenotype [11, 12, 14] and USP1 disruption or the absence of de-ubiquitination abrogates FancD2 foci formation and ICL repair and increases sensitivity to DNA cross-linkers [10–13].

Several studies have documented an interaction between HPV and the FA pathway. First, loss of FancA or FancD2 lead to hyperproliferation of HPV+ hyperplasia and increased proliferation of HPV genomes in organotypic cultures [15, 16]. Loss of FancD2 potentiates E7 driven cancers of the female lower reproductive tract, and head and neck in two separate studies using mouse models [17, 18]. Second, FA patients are susceptible to oral and anogenital squamous cell carcinomas [19], though the involvement of HPV in these cancers is controversial because of inconsistent detection of HPV DNA [20–23]. Third, HPV+ head and neck cancer cell lines show greater sensitivity to cisplatin compared to HPV negative cells [24].

The molecular mechanism(s) by which HPV interacts with the FA pathway is not well-understood. HR-HPV (mainly E7) was shown to upregulate several FA genes and activate the FA pathway by increasing FancD2 monoubiquitination and foci formation [25–27]. In contrast, HPV oncogenes were reported to perturb the functions of several FA proteins, including ATR, BRCA2/FancD1, BRCA1/FancS, and Rad51/FancR [3, 28–30]. Because HPV increases sensitivity to DNA crosslinkers [24], and a functional FA pathway restricts HPV replication [16], and FancD2 is preferentially recruited to the HPV episome leaving the cellular genome unrepaired [31], we hypothesized that HPV oncogenes impair the FA DNA repair pathway to facilitate the HPV life cycle. To date, studies have shown that HPV increases monoubiquitination of FancD2/ FancI [25–27, 31], but none have studied their deubiquitination pattern, which is as important as monoubiquitination for ICL repair [10–13]. Our study shows that HPV E6 caused delayed deubiquitination of FancD2 though it increased FancD2 monoubiquitination. Similarly, HPV E6 and E7 expressing cells increased FancD2 foci formation but impaired FancD2 colocalization to double-strand breaks. Collectively, our data demonstrate that HPV16 oncogenes abrogate the FA pathway, which further supports the hypothesis that HPV inhibits cellular DDR causing genomic instability.

Results

HPV16 oncogenes impair ICL repair and depend on the FA pathway for cisplatin sensitivity

We have previously shown that β-HPV 5/8 E6 and HPV16 E6 expression increases sensitivity to crosslinking agents such as cisplatin, mitomycin C and UVB [28]. To determine if the expression of E7 could also increase crosslinker sensitivity, we expressed HPV16 E6 and E7 individually or together in primary human foreskin keratinocytes (HFKs). Expression of HPV16 E6 and E7 was confirmed by qRT-PCR, as well as by immunoblot for their established targets p53 and pRB (S2 Fig). We found that both E6 and E7 expressing cells are hypersensitive to cisplatin compared to LXSN control (Fig 1A). When IC50 values were compared, E6 and E7 expressing cells were respectively 3.4 and 2 times more sensitive to cisplatin than LXSN.

Genetic epistasis analysis was conducted to determine whether the cisplatin hypersensitivity observed in E6/E7 expressing cells is due to a defect in the FA pathway. For this, we knocked down FancD2 and assessed cisplatin sensitivity (Fig 1B and 1C). FancD2 protein depletion by siRNA was confirmed by immunoblotting. FancD2 knockdown in LXSN control cells resulted in further increased sensitization to cisplatin, whereas there was little/no effect on cisplatin sensitivity in E6 or E7 expressing cells (Fig 1C). These results suggest that cisplatin sensitivity of HPV oncogene expressing cells is due to a defect in the FA pathway, particularly at or downstream of FancD2.

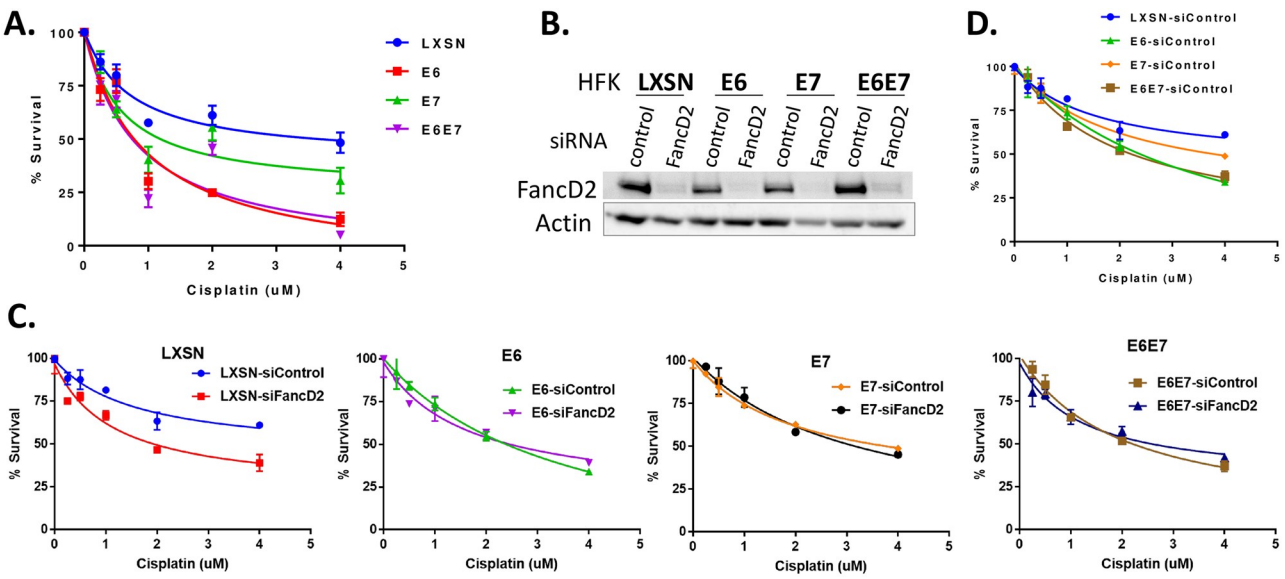

Fig 1. HPV oncogenes expressing cells impair ICL repair and depend on FancD2 for cisplatin sensitivity. (A) Cells were treated with increasing concentrations of cisplatin for 72 hr and % survival was measured using the Crystal Violet assay. LXSN, E6, E7, E6E7 expressing cells showed respective IC50 of 2.5, 0.74, 1.27 and 0.73 uM; 72 hr. (B-D) Cells were transfected with siControl or siFancD2 for 48hrs and plated for western blotting and cisplatin survival assay. (B) Western blot showing FancD2 knockdown in the cells harvested at the time of reading survival assay. (C) Survival curves of LXSN, E6, E7 and E6E7 cells transfected with siRNA (siFancD2 or siControl) and treated with indicated doses of cisplatin for 48 hr. (D) Survival curve of siControl cells treated with indicated doses of cisplatin for 48 hrs.

https://doi.org/10.1371/journal.ppat.1007442.g001

The ability of E6/E7 expressing cells to repair cisplatin-induced ICLs was investigated by utilizing a modified comet assay which has been widely used to evaluate ICL repair *in vivo* at the single cell level [32–34]. Cells were treated with cisplatin for 2 hr and then incubated in cisplatin-free medium. At 24, 48 and 72 hours post-treatment, cells were harvested and frozen to analyze all samples concurrently. Cells were thawed and irradiated to deliver a fixed level of random DSBs immediately prior to the comet assay (Fig 2A). Crosslinks hold the two strands of DNA together during alkaline denaturation and retard electrophoretic mobility of the irradiated DNA resulting in a reduced tail moment compared to untreated irradiated controls. The tail moment, which takes into account both tail length and amount of DNA in the tail, was at a basal level in untreated and unirradiated cells (Fig 2B). At 0 hr post-cisplatin treatment, the tail moment was decreased in all cell types compared to corresponding irradiated untreated controls. At 72 hr post-cisplatin treatment, LXSN cells regained the tail moment indicating that these cells were able to repair crosslinks. In contrast, E6E7 expressing cells did not improve the tail moment 72 hr after cisplatin treatment, suggesting that ICLs remained unrepaired in these cells (Fig 2C). Further, repair kinetics of cisplatin-induced ICLs were expressed as the percentage of crosslinks remaining at the time points assessed (Fig 2C). ICLs present in the cisplatin-treated sample were calculated by comparing the tail moment of treated and irradiated (Cp.IR) cells with irradiated (IR) samples and untreated (Ø) control samples (as described in Methods). Cisplatin-induced ICLs were removed efficiently in LXSN cells with ~35% of the ICLs remaining at 72 hr, whereas in E6 or E7 expressing cells, significantly elevated levels of ICLs persisted and remained unrepaired even at 72 hr. Increased formation of % ICLs in E6/E7 cells at 24, 48 and 72 hr may be due to inefficient removal of the DNA-platinum monoadducts or intrastrand adducts by the repair system and their possible conversion to higher order adducts[35]. Taken together, these data support the hypothesis that HPV oncogene expressing cells have a decreased ability to repair cisplatin-induced ICL.

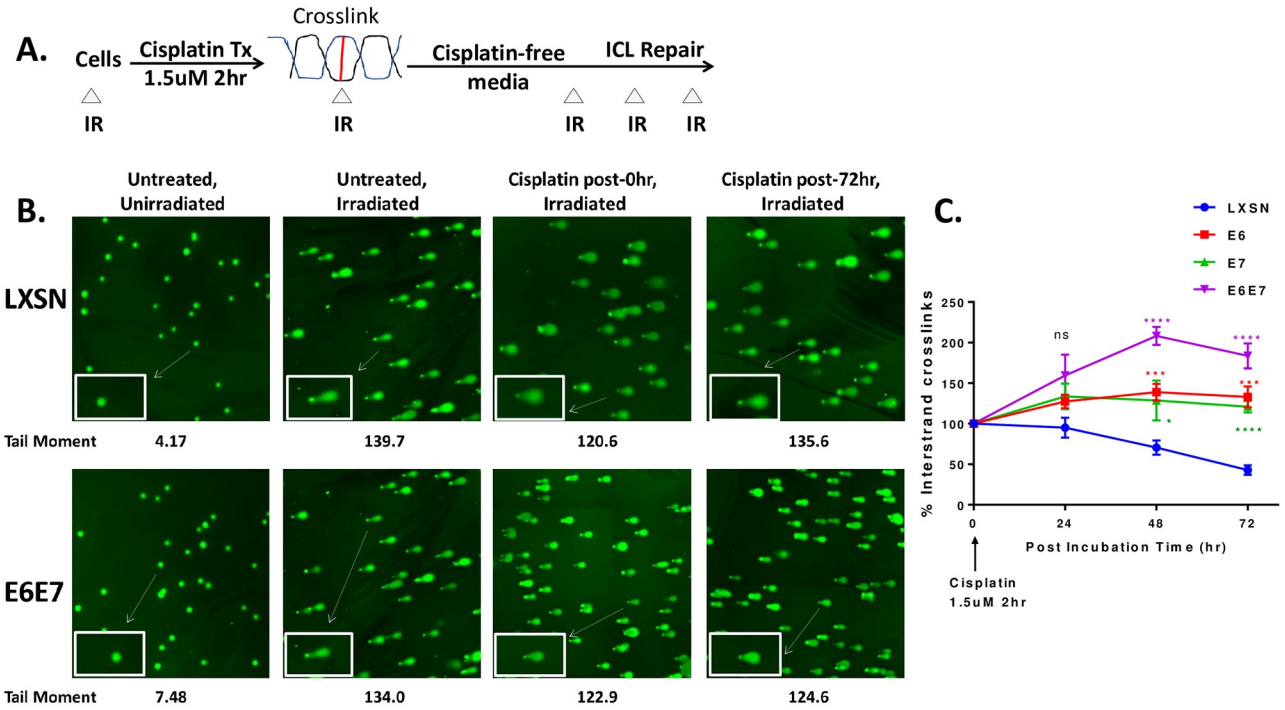

Fig 2. HPV oncogenes impair the repair of ICLs. (A) Outline of an experiment to evaluate repair of cisplatin-induced ICLs using the modified alkaline comet assay. Cells were treated with 1.5 μM cisplatin for 2 hr and then incubated in cisplatin-free medium. Triangles (Δ) represent the time points (0, 24, 48 and 72 hr after cisplatin release) when cells were harvested and frozen. Immediately before comet analysis, cells were thawed and irradiated with 12 Gy to deliver a fixed level of random DSBs. (B) Representative comet images of untreated and cisplatin treated+ irradiated cells at 0hr and 72 hr. The insets are the magnified comets. A mean tail moment from a representative assay is shown. (C) Quantification of % ICL present in LXSN and E6/E7 expressing HFK cells at different post-treatment incubation time. The percentage of ICLs remaining was determined as described in Methods. Data represent mean ± SEM of at least 3 independent biological replicates. * ($p < 0.05$), *** ($p \leq 0.001$), **** ($p < 0.0001$) denote a statistically significant difference from LXSN at the same post incubation time. 'ns' denotes non-significant differences.

https://doi.org/10.1371/journal.ppat.1007442.g002

FancD2/ FancI monoubiquitination is not impaired by HPV oncogenes

To screen for defects in the FA pathway, we first examined the levels of FancD2 in HPV oncogene expressing cells. When untreated cells were analyzed, total FancD2 (Ub + non-Ub) levels were significantly increased in E6/E7 expressing cells compared to LXSN control (Fig 3A). When E6 or E7 were individually expressed, cells had about 2 times more total FancD2 compared to LXSN; but the level increased by ~4 fold when E6 and E7 were expressed together. Total FancI (Ub + non-Ub) levels were also proportionately increased in E6/E7 expressing cells compared to LXSN.

FancD2 monoubiquitination was evaluated in E6/E7 expressing cells as a readout to define an activated FA pathway. Ub-FancD2 or Ub-FancI can be distinguished from the non-Ub form as a retarded mobility on gels. E6 and E7 increased FancD2 and FancI monoubiquitination both at baseline and after cisplatin treatment (Fig 3A). Approximately a 3-fold increase in the Ub-FancD2: non-Ub FancD2 ratio was observed in E6/E7 expressing cells on cisplatin treatment. Similar results were observed following MMC treatment and UVB irradiation (S2C and S2D Fig). When cells were analyzed following different lengths of cisplatin treatment, LXSN cells showed Ub-FancD2 after 6 hr of cisplatin treatment; but Ub-FancD2 was found in E6 cells even without cisplatin treatment (S2E Fig). Further, we performed cellular fractionation analyses and prepared chromatin and soluble fractions from HFKs expressing HPV oncogenes or LXSN control. As expected, Ub-FancD2 or Ub-FancI was enriched dramatically

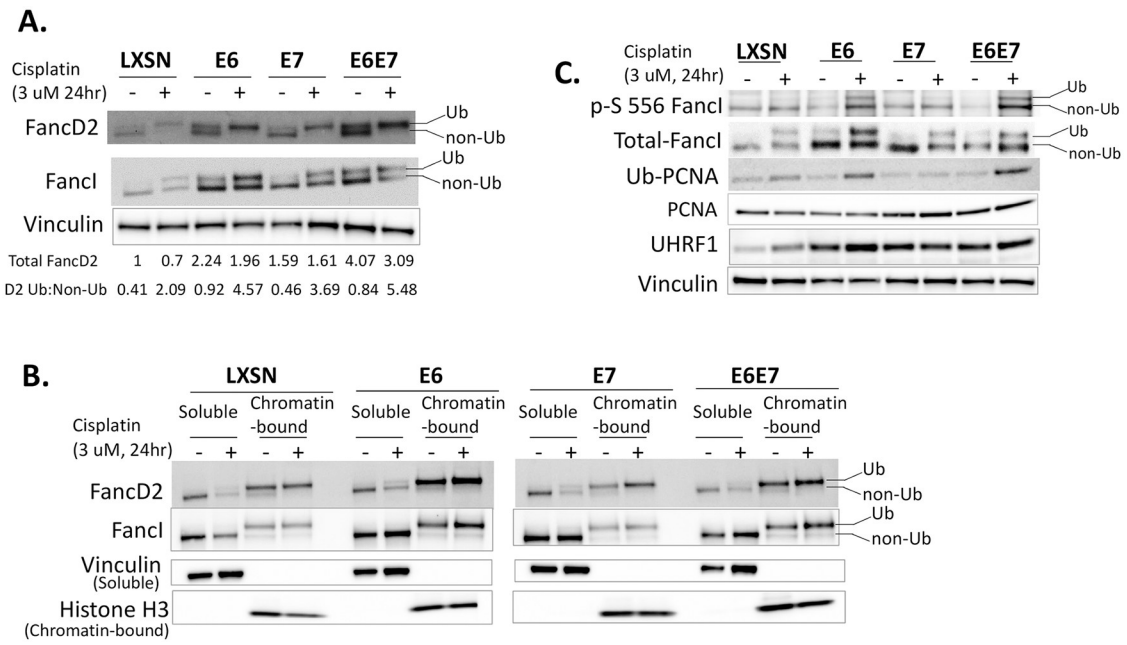

Fig 3. HPV oncogenes increase chromatin-bound monoubiquitinated FancD2/ FancI. (A) Immunoblot showing FancD2/ FancI expression and monoubiquitination status in transduced HFK cells which were either untreated or treated with 3 uM cisplatin for 24 hr. Ub refers to the monoubiquitinated forms of FancD2 and FancI, and non-Ub refers to the non-ubiquitinated forms. Ratios of monoubiquitinated to non-ubiquitinated FancD2 (D2 Ub: Non-Ub) and total FancD2 (Ub + Non-Ub) levels are indicated beneath the corresponding lanes. (B) Immunoblot of soluble and chromatin-bound fractions prepared from transduced HFK cells that were either untreated or treated with 3 uM cisplatin for 24 hr. Vinculin and Histone H3 act as loading controls respectively for soluble and chromatin-bound fractions. (C) Immunoblot of whole cell lysates showing levels of phosphorylated S556 FancI, total FancI, Ub-PCNA, non-Ub PCNA, and UHFR1. Vinculin acts as a loading control.

https://doi.org/10.1371/journal.ppat.1007442.g003

in the chromatin-bound fraction of all transduced HFK cells. Importantly, an increased recruitment of Ub-FancD2/ FancI to chromatin was detected in E6 expressing cells compared to LXSN control and E7 expressing cells (Fig 3B).

We next wanted to determine whether high levels of FancD2 and FancI in E6 expressing cells were due to increased transcription or greater protein stability or both. No significant differences in FancD2 mRNA levels between LXSN and E6/E7 expressing cells were observed (S3A Fig). To determine protein stability, cells were exposed to the translation inhibitor cycloheximide (CHX) and protein levels were monitored over a 24 h period (S3B). LXSN showed a rapid FancD2 turnover with half-life (t ½) of ~3 hr and diminished to low levels in 24 hr after CHX addition. In contrast, E6 expressing cells had the t ½ of >24 hr and FancD2 levels remained elevated 24 hr following the addition of CHX. One study reported that the mono-ubiquitination of FancD2 promotes its stabilization in chromatin and cells that are deficient in monoubiquitination has significantly reduced FancD2 protein half-life [36]. Increased FancD2 stability in E6 cells may be due to high levels of mono-ubiquitinated form of FancD2 in these cells. FancI mRNA levels were significantly elevated in E6/E7 expressing cells compared to LXSN (S3A Fig). Consistently, the turnover rate of total FancI was considerably delayed in E6 cells compared to LXSN (S3B-C).

We next sought to know the effectors that may contribute to increasing FancD2 monoubiquitination in E6/E7 expressing cells. Phosphorylation of FancI S556 occurs upstream of, and enhances, FancD2 monoubiquitination [7]. Additionally, the proliferating cell nuclear antigen (PCNA) is monoubiquitinated by the RAD18 ubiquitin ligase in response to ICL lesions. Apart from its role in translesion synthesis repair, ubiquitinated PCNA (PCNA-Ub) is known

to promote FancD2 monoubiquitination by either facilitating FancD2 recruitment onto chromatin via a direct physical interaction [36] or by promoting the recruitment of FancL and its E3 ubiquitin ligase activity on FancD2 [37]. Further, the protein UHRF1 (ubiquitin-like with PHD and RING finger domains 1) has recently been identified as a sensor of ICLs and is required for the recruitment of FancD2 to ICL sites [38, 39]. Phosphorylated FancI-S556, Ub-PCNA, and UHFR1 levels were increased in E6 expressing cells compared to LXSN following cisplatin treatment (Fig 3C). Elevated UHRF1 levels in E6 cells was the consequence of upregulation of UHRF1 transcription and decreased protein turnover rate (S3A–S3C Fig).

Depletion of ATR by siRNA knockdown decreased the phosphorylation of FancI at S556 and therefore reduced the Ub-FancD2 level (S4A and S4D Fig), suggesting a role for p-556 FancI in increasing the chromatin-bound fraction of Ub-FancD2 in E6 cells. On the other hand, depletion of UHRF1 did not reduce Ub-FancD2 level in E6 cells (S4B and S4E Fig), indicating elevated UHRF1 may not be involved in increasing Ub-FancD2. When PCNA was depleted, FancD2 was mono-ubiquitinated even in untreated E6 cells (S4C and S4F Fig). A report shows that RAD18, which ubiquitinates PCNA, plays a significant role in monoubiquitination of FancD2 even in the absence of PCNA [40]. Consistent with this report, our data indicates that Ub-PCNA is not essential in increasing Ub-FancD2 level in E6 expressing cells.

HPV oncogenes do not disrupt FancD2 nuclear foci formation but impair colocalization of FancD2 with double-strand DNA breaks

To further investigate the interaction of HPV with the FA pathway, the ability of E6/E7 expressing cells to form nuclear foci of FancD2 was quantified as the percentage of cells with >5 FancD2 foci in HFKs. FancD2 foci formation in cisplatin-treated E6 or E7 cells was elevated compared to LXSN controls (Fig 4A and 4B). Even without cisplatin treatment, there was increased FancD2 foci formation in E6 expressing cells. Phospho-H2AX foci were used as markers for DNA double-strand breaks (DSB).

We previously reported that HPV oncogene expressing cells impair the colocalization of Rad51 with pH2AX [3]. The same approach was used to investigate whether E6/E7 expressing cells affect the localization of FancD2 to DSBs. The expression of HPV oncogenes caused FancD2 to be localized away from DSBs (Fig 4A). In cells expressing E6 or E6+E7, only ~50% of FancD2 appeared to co-localized with pH2AX. E7 expressing cells showed a modest (~25%) but statistically significant reduction in colocalization of FancD2 to pH2AX compared to LXSN (Fig 4C). To complement these co-localization studies, we utilized U2OS-DR cells transduced with LXSN, E6, E7 and E6E7 and transiently transfected with an I-SceI expression vector, as previously described [3]. These U2OS cells have clonally integrated DR-GFP cassette consisting of two copies of nonfunctional GFP (S5A Fig) [41]. Exogenous expression of I-SceI produces a single DSB within the first GFP gene which contains an I-SceI recognition site. Thus, cells with single large pH2AX foci were selected and inspected for its colocalization with FancD2 (S5A Fig). An excellent colocalization of FancD2 with pH2AX was observed in LXSN cells, but there was ~50% and 20% reduction in colocalization of FancD2 in E6 and E7 expressing cells, respectively compared to LXSN cells (Fig 4D and 4E). These data suggest that FancD2 is forming repair complexes by localizing away from DSBs in E6/E7 expressing cells. Because E6/E7 induce replicative stress (data in progress), one possibility is that FancD2 complexes are localizing to single strand DNA breaks or stalled replication forks.

FancD2 is responsible for Rad51 mislocalization in E6 cells

Mislocalization of FancD2 in E6 cells (Fig 4D and 4E) may hinder the recruitment of downstream proteins, such as Rad51 to sites of DNA damage. In fact, several lines of evidence

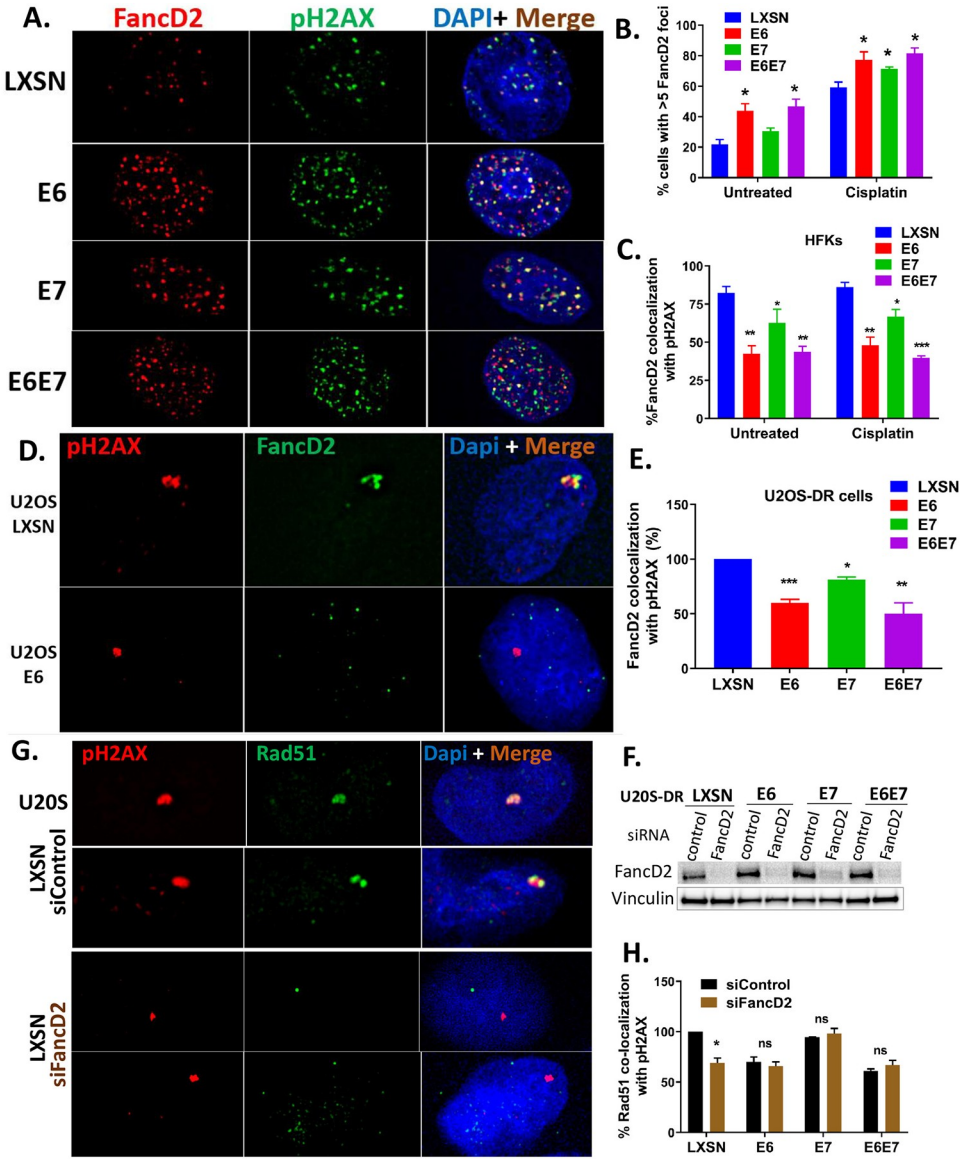

Fig 4. HPV oncogenes increase FancD2 foci formation but impair colocalization of FancD2 with DSBs, and mislocalized FancD2 in E6 cells causes reduction in Rad51 recruitment to DSBs. (A) HFK cells were treated with cisplatin (3 uM) for 24 hr and immunostained with FancD2 (red), pH2AX (green) and DAPI (blue). Representative images are shown. (B) Cells with >5 foci were counted, and the percentage of positive cells is plotted (n = 3, mean ± SEM). (C) Quantification of percentage of FancD2 foci co-localization with pH2AX with or without cisplatin treatment. * (p-value ≤ 0.05) and ** (p-value ≤ 0.01) denote a statistically significant difference from the similarly treated LXSN control cells. Error bars represent standard error of the mean. Quantification was based on data observed from ≥ 15 nuclei from three independent experiments. (D) U2OS-DR cells (transduced with LXSN or E6/E7) were transfected with I-SceI expression plasmid for 24 hr before fixation. Cells were immunostained with pH2AX, FancD2, and DAPI (blue). Cells with a single large pH2AX focus (red) were examined for the colocalization with FancD2 (green). Representative images are shown. (E) Quantification of the frequency of colocalization of FancD2 with pH2AX foci in U2OS-DR cells. Data represent mean ± SEM and was based on observations from ≥ 50 cells from at least three independent experiments. (F-H) U2OS-DR cells transduced with the indicated constructs were transfected with the siControl or siFancD2. They were transfected with I-SceI expression plasmid and then fixed after 24 hr of transfection and stained with Rad51 and pH2AX antibodies. (F) Cell lysates were subjected to western blotting to confirm depletion of FancD2. (G) Cells with a single large pH2AX focus (red) were inspected for the colocalization with Rad51 (green). Representative images are shown. (H) Quantification of the frequency of colocalization of Rad51 with pH2AX foci. Data represent mean ± SEM and was based on observations from ≥ 25 cells from at least three independent experiments. * and ** indicate significance respectively at $p<0.05$ and $p<0.01$ (compared to LXSN) whereas n.s. indicates non-significant.

https://doi.org/10.1371/journal.ppat.1007442.g004

indicate that FancD2 helps in the localization of Rad51 to DSBs. First, Ub-FancD2 colocalizes with Rad51 in nuclear foci during S phase [42]. Second, FancD2 promotes recruitment of Rad51 in nuclear foci by directly binding and stabilizing Rad51-DNA nucleoprotein filament for DSB repair [43, 44]. Third, FancD2 colocalized with Rad51 in cisplatin treated HFK LXSN control cells (S5B Fig). We previously reported that the colocalization of Rad51 with DSB is impaired in E6 expressing cells [3]. To determine whether the mislocalization of Rad51 observed in E6 expressing cells is epistatic to FancD2, the Isce-I colocalization assay was repeated, as described above (Fig 4C), in FancD2-depleted cells and immunostained with Rad51 and pH2AX. Western blot analysis confirmed FancD2 protein depletion in the siFancD2-transfected cells compared to siControl cells (Fig 4F). FancD2 depletion in LXSN cells caused a modest (~20%) but statistically significant reduction in colocalization of Rad51 to pH2AX in I-SceI induced DSB (Fig 4G and 4H), supporting the idea that FancD2 promotes Rad51 recruitment to DSB in normal cells. However, in E6 expressing cells, there was no further significant reduction in colocalization of Rad51 to pH2AX on FancD2 knockdown, suggesting that the Rad51 recruitment defect associated with E6 cells is due to FancD2.

HPV E6 causes delayed de-ubiquitination of FancD2

To further screen for defects in the FA pathway, we investigated how E6/E7 affects the de-ubiquitination pattern of FancD2/ FancI upon DNA repair. Though FancD2/ FancI monoubiquitination is considered as a functional activator of the FA pathway, de-ubiquitination of FancD2/ FancI is also critical for effective ICL repair [10–13]. Since E6/E7 increases monoubiquitination of FancD2/ FancI, there may be a defect in de-ubiquitination. To address this, cells were treated with cisplatin or exposed to UV and allowed to recover for the indicated time (Fig 5A). Delayed de-ubiquitination of FancD2 was observed in E6 expressing cells during recovery after UVB exposure or cisplatin removal (Fig 5A–5C). Most of FancD2 was de-ubiquitinated following 24 hr of UVB and cisplatin release in LXSN cells but not in E6 or E6+E7 expressing cells. E7 expressing cells behaved more like LXSN.

As Ub-FancD2 persists abnormally in E6 cells, a series of experiments were designed to determine the basis of the delay in de-ubiquitination. First, we asked whether this phenotype was a consequence of decreased levels of the FancD2 deubiquitinating enzyme, USP1. In fact, the opposite result was obtained: E6/E7 expressing cells showed elevated USP1 with cisplatin treatment, while basal levels of USP1 did not differ among untreated cells (Fig 5D). These results suggest that delayed FancD2 de-ubiquitination in E6 cells is not because of lower USP1 expression. Second, a recent study indicated that de-ubiquitination of FancD2/ FancI by USP1 occurs only when the complex is no longer bound to chromatin [45]. Delayed FancD2 de-ubiquitination in E6 expressing cells may be due to retaining a chromatin-bound conformation of FancD2/FancI after DNA damage. To address this possibility, the association of FancD2/FancI with chromatin was examined using cell fractionation following cisplatin withdrawal or UVB exposure (Fig 5E). 24 or 48 hr following UVB exposure, E6 or E6+E6E7 expressing cells showed increased chromatin-bound Ub-FancD2/ FancI, whereas LXSN and E7 expressing cells showed predominantly soluble non-Ub FancD2/I. There was also increased chromatin-bound Ub- FancD2/ FancI at 18 and 24 hr following cisplatin treatment in E6 expressing cells compared to LXSN control. These data suggest that the delayed de-ubiquitination pattern observed in E6 expressing cells was due to FancD2/ FancI being retained in a chromatin-bound conformation where USP1 cannot work efficiently to de-ubiquitinate the complex, despite high levels of USP1.

Third, while FancI phosphorylation at Serine 556 promotes FANCD2 monoubiquitination, its phosphorylation at Serine 565 inhibits FANCD2 de-ubiquitination and impairs ICL repair

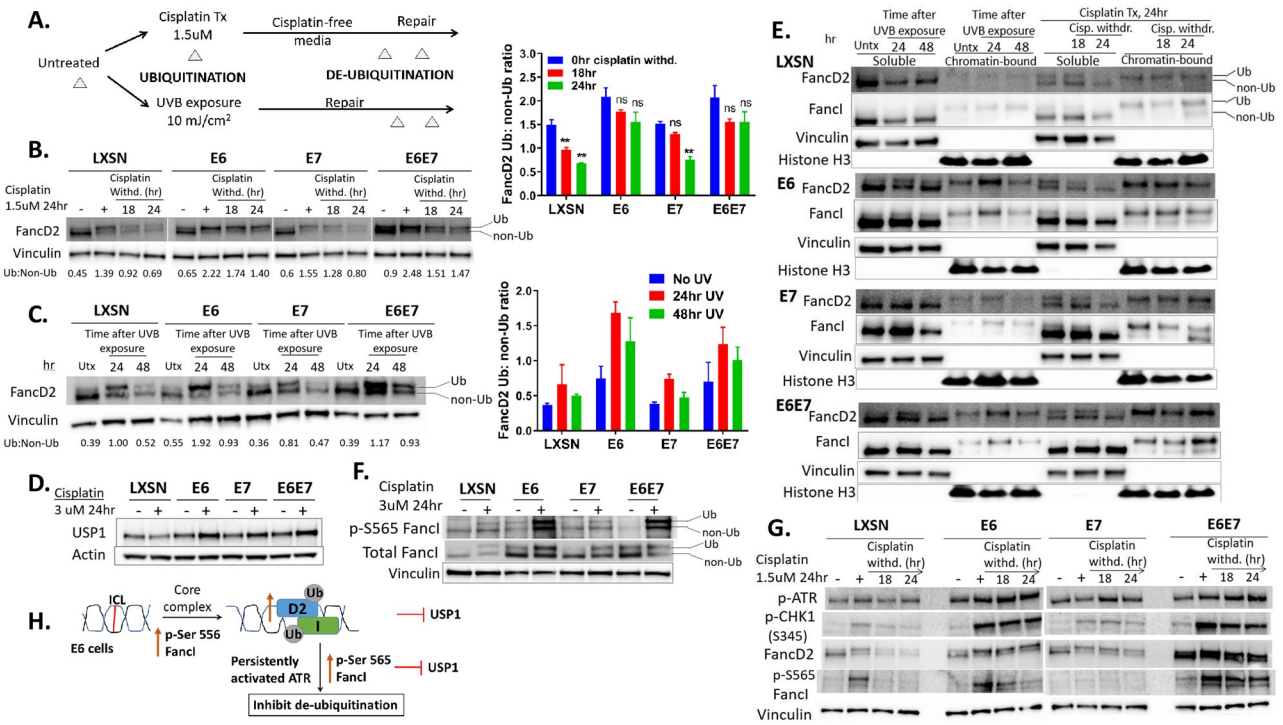

Fig 5. HPV E6 causes delayed de-ubiquitination of FancD2. (A) Outline of an experiment to evaluate FancD2 monoubiquitination/de-ubiquitination pattern. Transduced HFK cells were untreated or treated with cisplatin (1.5 uM for 24 hr) or exposed to 10 mJ/cm^2 UVB and allowed to repair. Whole-cell lysates were prepared for immunoblot at various time points during the experiments (represented by Δ). (B-C) Immunoblots of HFKs subjected to the experiment outlined in Fig 4A, following cisplatin withdrawal (B) or recovery after UVB exposure (C). Ratios of monoubiquitinated to non-ubiquitinated FancD2 (D2 Ub: non-Ub) are indicated beneath the corresponding lanes. FancD2 Ub:non-Ub ratio in cells following cisplatin withdrawal and UVB exposure was plotted alongside Figure 5B and 5C. ** ($p < 0.01$) denotes a statistically significant difference from 0 hr cisplatin withdrawal. 'ns' denotes non-significant differences. (D) USP1 immunoblot in cells untreated and treated with cisplatin. (E) Immunoblot of soluble and chromatin-bound fractions prepared from transduced HFK cells subjected to the experiment outlined in Fig 6A. Vinculin and Histone H3 act as loading controls respectively for soluble and chromatin-bound fractions. (F) Immunoblot showing levels of p-FancI-S565 and total FancI in cisplatin-treated or untreated cells. (G) Immunoblot for p-ATR, pCHK1, FancD2 and p-FancI-S565 following cisplatin withdrawal for 18 and 24 hrs. Actin or vinculin act as a loading control for immunoblots (B-G). (H) Proposed mechanisms for delayed de-ubiquitination of FancD2 in E6 cells.

https://doi.org/10.1371/journal.ppat.1007442.g005

[7]. Therefore, we investigated whether delayed de-ubiquitination of FancD2 was also due to elevated levels of phosphorylated-S565 FancI in E6 expressing cells. As expected, E6 or E6+E7 expressing cells showed increased p-S565 FancI on cisplatin treatment (Fig 5F). As phosphorylation of FancI occurs through the ATR-mediated pathway [7] and ATR/CHK1 activation increases FancD2 monoubiquitination [9], delayed FancD2 deubiquitination in E6 cells may be due to persistently activated ATR. Therefore, we examined the levels of p-ATR, p- S345 CHK1, p-S565 FancI as well as FancD2 monoubiquitination/ deubiquitination patterns in cells which had recovered for 24 hr in normal media after cisplatin withdrawal. In E6 or E6+E7 expressing cells, ATR/CHK1 was activated and persisted following cisplatin withdrawal, compared to LXSN (Fig 5G). These results are consistent with persistent levels of both ubiquitinated FancD2 and S565-phosphorylated FancI in E6 expressing cells following cisplatin release. Further, persistence of pATR foci and pCHK1 following UV exposure was seen in E6 cells compared to LXSN (S6A and S6B Fig). In E6 expressing cells, an ATR specific inhibitor (VE821) following cisplatin withdrawal caused an increase in FancD2 de-ubiquitination (Ub: non-Ub ratio of 0.6 and 0.51 at 18 and 24 hrs of VE821 treatment compared to a ratio of 1.74 and 1.40 at same time points in normal media), S6C and S6D Fig. These data demonstrate that

persistently activated ATR/pCHK1/pFancI signaling could contribute to the delayed de-ubiquitination of FancD2 in E6 cells. Fig 5H shows the potential mechanisms for delayed de-ubiquitination of FancD2 in E6 cells.

E6 does not abrogate the cell-cycle specific process of FancD2 monoubiquitination or de-ubiquitination

To determine whether the effect of E6 on increased monoubiquitination and delayed de-ubiquitination of FancD2 was a consequence of aberrant cell cycle progression, LXSN and E6 cells were synchronized in early S-phase by double-thymidine block, released, and FancD2 mono- or de-ubiquitination patterns were examined as cells progressed through the cell cycle (Fig 6). A previous study reported that FancD2 undergoes monoubiquitination during the S-phase of the cell cycle [4]. Consistent with this study, in both LXSN and E6 cells, monoubiquitinated FancD2 was the major isoform present upon release from double-thymidine arrest into G1/S border and S-phase. Ub-FancD2 was noticeable till late S-phase, just prior to the decline of cyclin A. It is known that USP1 deubiquitinates FancD2 when cells exit S phase [12]. Ub-FancD2 was de-ubiquitinated when both LXSN and E6 cells exited S phase. Cell-cycle analysis by flow cytometry was performed at each time point to track cell-cycle progression (Fig 6D). These data suggest that E6 does not abrogate cell cycle-specific process of FancD2 monoubiquitination and de-ubiquitination.

E6 mediated increased FancD2 monoubiquitination is p53 independent

To further address the regulation of FancD2 mono or de-ubiquitination, the potential role of p53 was examined. The p53 tumor suppressor is a major cellular target of HPV16 E6. One study reported that p53 downregulates FancD2 mRNA and protein levels [46]. As E6 degrades p53, we expected to see increased FancD2 mRNA and protein levels in E6 expressing cells. However, no significant differences in FancD2 mRNA levels between LXSN and E6 cells were observed (S3A Fig). But, since there was increased protein levels of total FancD2 in E6 expressing cells (Fig 3A), we hypothesized that this phenotype was dependent on the ability of E6 to degrade p53. To test this, HFK cells expressing a mutant of HPV16 E6 (8S/9A/10T) that is incapable of degrading p53 [47, 48] was used. Western blot analysis confirmed that E6 expression degrades p53, but the mutant failed to induce p53 degradation (Fig 7A, upper panel). Both cell lines were also evaluated for E6 expression by RT-PCR (Fig 7A, lower panel). Total FancD2 level was similar in mutant E6 and wild-type E6 cells (Fig 7B), indicating that E6 increased FancD2 protein level independently of its effects on p53 degradation. To confirm these results, cells were treated with Nutlin-3a, a Mdm2 inhibitor that increases p53 activity by preventing Mdm2-mediated proteasomal degradation. Nutlin treatment decreased total FancD2 level in LXSN cells but not in E6 expressing cells (Fig 7C). Similar downregulation of FancD2 was observed in lung fibroblast cells upon Nutlin-induced p53 activation, with no significant change in FancD2 level in p53-deficient counterparts [46].

Several publications suggested that FancD2 monoubiquitination is p53-independent. Several p53 defective cancer cell lines and chicken B lymphocyte cells lacking functional p53 were found to be fully competent for FancD2 monoubiquitination [49–51]. Interestingly, Rego et al. showed that FancD2 mono-Ub is p53-independent but dependent on p21, its downstream target [49]. In our study, although E6 showed increased Ub-FancD2 compared to LXSN, this increment was similar in mutant E6 cells, which fail to degrade p53 (Fig 7B). Hence, increased monoubiquitination of FancD2 by E6 is not a direct consequence of p53 degradation. To confirm these results, we used p53 knockdown LXSN cells and found that the Ub-FancD2 level was unchanged when compared to p53-sufficient LXSN (S7 Fig).

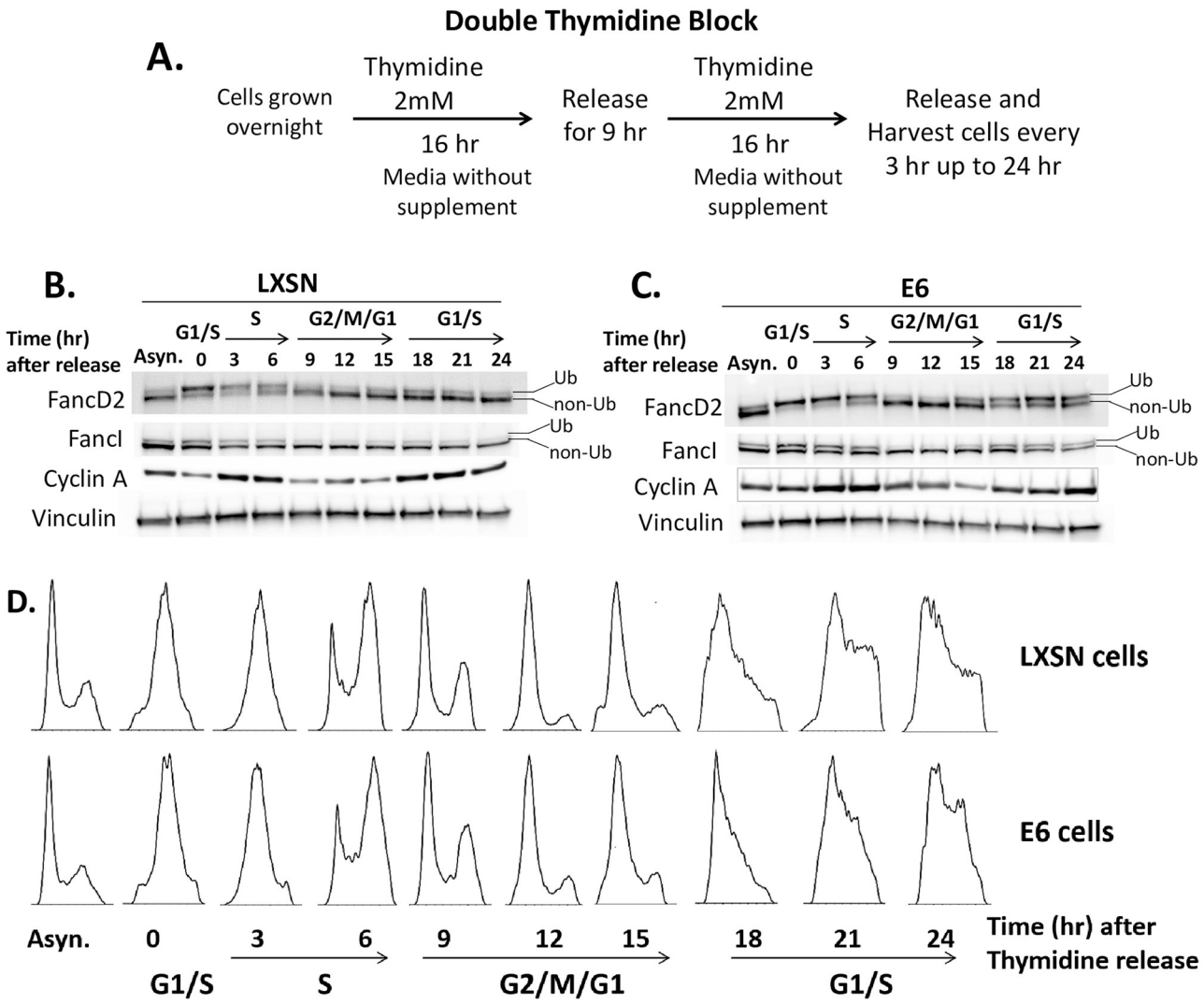

Fig 6. Cell-cycle specific process of FancD2 monoubiquitination/ de-ubiquitination is not abrogated in E6 cells. (A) Outline of synchronization assay in HFK cells using double-thymidine block. Cells were synchronized by double-thymine block and released at various time points. Immunoblot for FancD2, FancI, cyclin A and vinculin of LXSN (B) and E6 cells (C). Cell-cycle phases at each time point were determined by flow cytometry of DNA content (D). Asynchronous (Asyn.) cells, which have not undergone thymidine block, were included for comparison.

https://doi.org/10.1371/journal.ppat.1007442.g006

E6 mediated delayed FancD2 de-ubiquitination is dependent on p53 degradation

The exact role of p53 in FancD2 de-ubiquitination is not well-understood, although a study reported that p21, a p53 downstream target, represses USP1 transcription [49]. Since E6 increased USP1 protein expression on cisplatin treatment (Fig 5D), we argued that the mechanism by which E6 causes delayed FancD2 de-ubiquitination may be related to its effects on p53 degradation. To examine this, we performed similar experiments as in Fig 5A in cells expressing the mutated E6 that is incapable of degrading p53. At 48hr after UV exposure, FancD2 de-ubiquitination pattern in mutant E6 was similar to LXSN control cells (Fig 7D, lanes 3 and 9). Similarly, after 24hr release from cisplatin treatment, mutant E6 showed de-ubiquitinated FancD2 (Ub: Non-Ub ratio of 0.67), whereas wild-type E6 cells had predominately

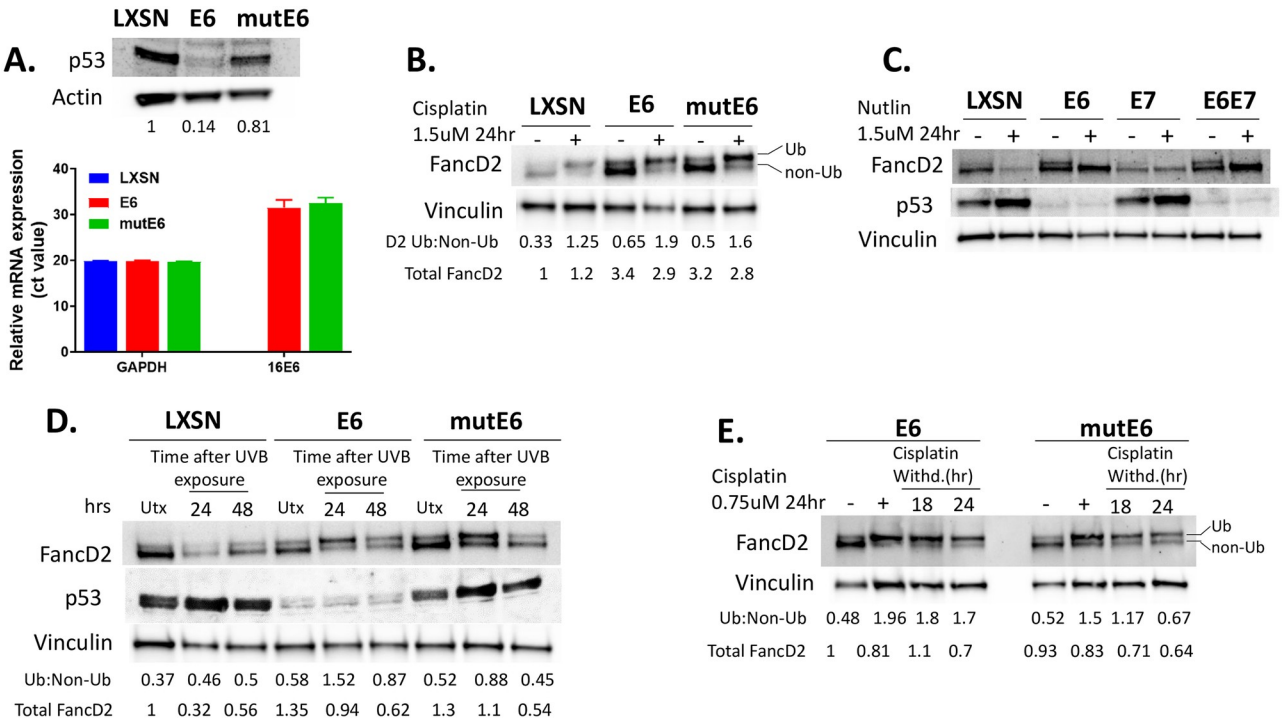

Fig 7. E6 mediated increased FancD2 monoubiquitination is p53 independent, but delayed FancD2 de-ubiquitination is dependent on p53 degradation. (A) Immunoblot for p53 (upper panel) and RT-PCR analysis of 16E6 and GAPDH expression (lower panel) in HFK cells transduced with LXSN, E6 and E6 mutant (8S/9A/10T). (B-C) Immunoblot showing FancD2 expression and monoubiquitination status in cells which were either untreated or treated with cisplatin (B) or nutlin (C) at 1.5 uM for 24 hr. (D-E) Cells were untreated or treated with cisplatin (E) or exposed to 10 mJ/cm^2 UVB (D) and processed similarly as in Fig 5.

https://doi.org/10.1371/journal.ppat.1007442.g007

monoubiquitinated FancD2 (ratio of 1.7) (Fig 7E). This indicates that delayed FancD2 de-ubiquitination in E6 cells was related to the ability to degrade p53. To confirm that the observed effects were specific consequences of p53 degradation, we used shRNA to stably knockdown p53 in LXSN cells and analyzed FancD2 Ub/de-Ub pattern upon UV exposure or cisplatin withdrawal. Once again, FancD2 de-ubiquitination was markedly delayed in the absence of p53 (S8B Fig). These results strongly support a p53-dependent effect of E6 in causing delayed FancD2 de-ubiquitination.

We next examined whether p53 dependent delayed FancD2 deubiquitination in E6 cells is due to activated ATR/CHK1/pFancI signaling. pATR/pCHK1 levels were reduced in cells expressing mutant E6 that cannot degrade p53 compared to wild-type E6 cells (S8C Fig). Reduction in ATR activity resulted in decreased phosphorylation of FancI at S565 and increased FancD2 de-ubiquitination in mutant E6 cells.

E6 attenuates Palb2 expression and foci formation

To further understand how E6 or E7 impair the FA pathway and cause genomic instability, the expressions of proteins downstream of FancD2/I complex were evaluated. As a key regulator of the FA pathway, FancD2 recruits and coordinates functions of downstream FA repair proteins [52], including BRCA2/FancD1, BRCA1/FancS, Rad51/FancR, Palb2/FancN and BRIP1/FancJ. Previously, we demonstrated that neither BRCA2, BRCA1 nor Rad51 protein expression is impaired by the HPV oncogenes [3]. To determine whether the abundance of any other downstream protein is affected by HPV oncogenes, the levels of Palb2 were measured. Palb2

level was reduced when E6 was expressed separately or together with E7 (Fig 8A). Reduced Palb2 protein in E6 expressing cells was not caused by downregulation of Palb2 transcription but was due to increased protein turnover (S9C and S9D Fig). E6 exhibited shorter half-life (t ½) of ~12 hr compared to LXSN with t ½ of >24 hr. Depleted Palb2 level in E6 cells was not a consequence of p53 degradation (S9B Fig). Because E6 reduced Palb2 levels, the ability of Palb2 to form nuclear foci in response to cisplatin was examined. In LXSN control cells, the percentage of cells with >5 Palb2 foci peaked at about 90% following cisplatin treatment. In contrast, significantly fewer (~60%) E6 expressing HFKs formed Palb2 foci on cisplatin treatment (Fig 8B). Although fewer Palb2 foci were observed in E6 cells, these foci perfectly localize to pH2AX in I-SceI transfected U2OS-DR system (S10A Fig). Because E6 reduces Palb2 expression and foci formation, and Palb2 is also a component of FA nuclear foci for ICL repair, we asked whether the cisplatin hypersensitivity observed in E6 expressing cells is due to a defect in Palb2. Genetic epistasis analysis for cisplatin sensitivity was conducted by knocking down Palb2. Palb2 depletion in LXSN and E7 cells resulted in further sensitization to cisplatin (Fig 8C), whereas there was no effect on cisplatin sensitivity in E6 and E6+E7 expressing cells. These results suggest that cisplatin sensitivity seen in E6 expressing cells is, in part, due to a defect in Palb2 expression and foci formation.

Reduced Palb2 expression and foci formation in E6 cells (Fig 8A and 8B) may affect the interaction of Palb2 with other FA repair proteins, such as Rad51, required for resolution of ICLs. In fact, Palb2 physically and functionally interacts with Rad51. First, Palb2 colocalizes

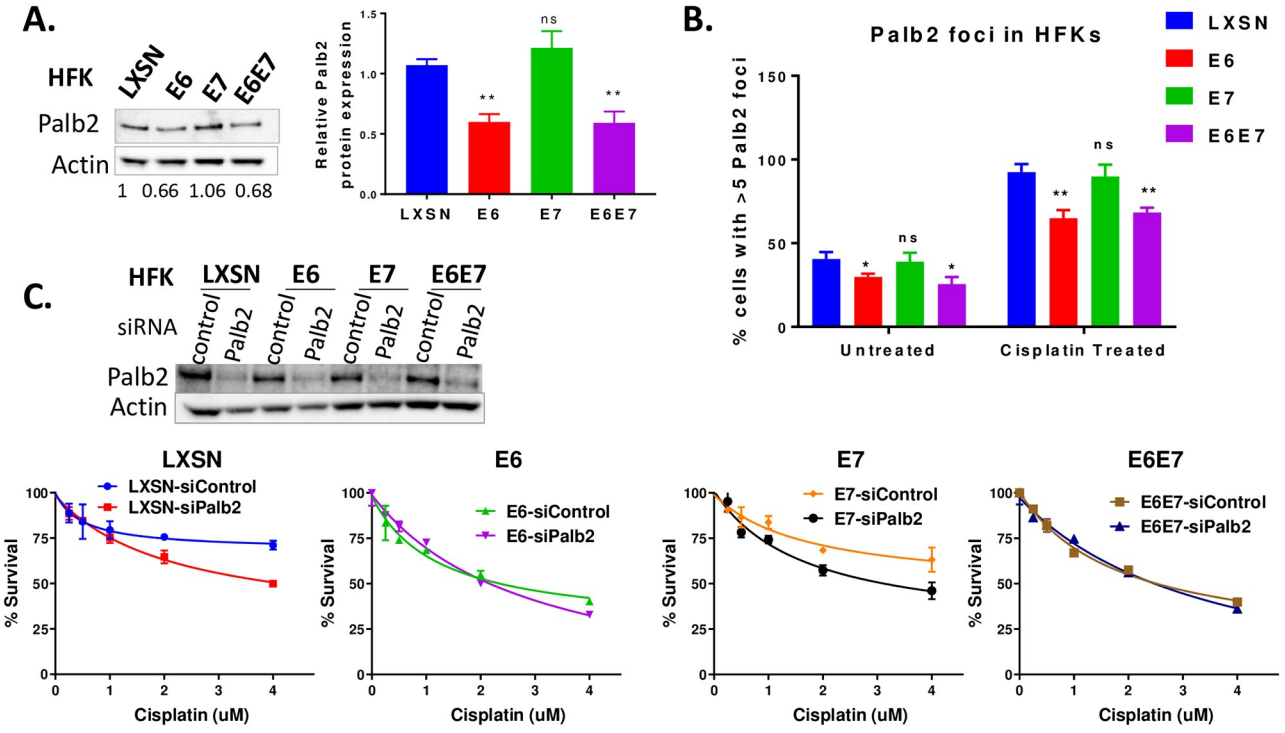

Fig 8. E6 attenuates Palb2 expression and foci formation. (A-C) HFKs were transduced with LXSN, E6 or E6/E7 (A) Immunoblot showing Palb2 expression. Actin serves as a loading control (left panel). Graph showing relative Palb2 protein expression from 3 independently derived E6/E7 cell lines (right panel). (B) Cells were untreated or treated with cisplatin (3 uM) for 24 hr and immunostained with Palb2, pH2AX, and DAPI. Cells with >5 Palb2 foci were counted and the percentage of positive cells is plotted (n = 3, mean ± SD). * and ** indicate significance respectively at $p<0.05$ and $p<0.01$ (compared to LXSN) whereas ns indicates non-significant. (C) HFKs were transfected with siControl or siPalb2. Immunoblot confirming depletion of Palb2 (upper panel). Cisplatin survival assay for siRNA-transfected cells (lower panel).

https://doi.org/10.1371/journal.ppat.1007442.g008

with BRCA2 foci, which also includes Rad51 [53–56]. Second, loss of Palb2 impairs Rad51 focus formation [57] and there is Palb2-dependent loading of BRCA2-Rad51 repair machinery at DSBs [56]. Therefore, we next examined whether the defect in localization of Rad51 observed in E6 expressing cells is due to decreased Palb2 expression or foci formation. In all HFK cells, including E6 expressing cells, Palb2 depletion caused a dramatic reduction in colocalization of Rad51 to pH2AX in I-SceI induced DSB (S10B Fig) indicating that the Rad51 recruitment defect observed in E6 cells is not due to impaired Palb2 expression and foci formation.

Discussion

The FA DNA repair pathway is involved in guarding genome integrity, especially when challenged by endogenous and exogenous DNA crosslinking agents. Cisplatin is the most commonly used chemotherapeutic drug for cervical and oropharyngeal cancers. Here we provide mechanisms by which HPV oncoproteins attenuate the FA pathway and contribute to tumorigenicity and the response to cisplatin therapies in HPV-associated malignancies. Our present study (Fig 1) along with others [24] confirm the cross-linker hypersensitivity in HPV oncogene expressing cells. We also show that E6/E7 expressing cells have a defect in repairing cisplatin-induced ICLs (Fig 2). The epistatic analysis confirmed that ICL sensitivity in E6/E7 cells was due to a defect in FancD2 or downstream of FancD2 (Fig 1). However, FancD2 monoubiquitination and foci formation were increased in E6 or E7 cells (Figs 3 and 4), which is consistent with the previous work conducted in high-risk HPV+ and HPV oncogene expressing cells [25, 27, 31]. Further, high risk, but not low-risk, E7 was shown to increase FancD2 foci formation and activate the FA pathway [26, 27]. Strikingly, Ub-FancD2 was seen without cisplatin treatment in E6 expressing cells, which might be due to the presence of activated ATR which increases FancD2 monoubiquitination [9]. HPV oncogenes though, promoted the initiation of FA pathway by increasing FancD2 monoubiquitination and foci formation but hindered the completion of the repair by multiple mechanisms. E6 or E7 caused the accumulation of monoubiquitinated FancD2 at sites away from DNA damage. This subsequently hindered the recruitment of downstream protein Rad51 to DNA damage sites in E6 cells (Fig 4D–4H). Further, E6 mediated p53 degradation does not hamper cell cycle specific process of FancD2 modifications but abrogate the repair by delaying FancD2 de-ubiquitination (Figs 5–7). In addition, E6 reduced the expression and foci formation of Palb2 (Fig 8). Though there was a defect in FancD2 localization to DSBs in E6 cells, no mislocalization of Palb2 was observed, which is in support of a recent study reporting that FancD2 and Palb2 localize to DSBs independently of each other [58].

HPVs have been shown to recruit numerous cellular repair factors to their replication centers, mainly for HPV amplification [59–61]. Similarly, HPV E1 has been shown to interact with USP1-UAF1 complex to facilitate viral replication [62]. We speculate that increased Ub-FancD2 and foci formation may create an environment where FA repair proteins are readily available to support HPV replication. Consistent with our speculation, a study showed that higher levels of FancD2 and larger foci are predominantly recruited to HPV DNA rather than cellular genomes and localize to viral replication centers [31]. The preferential recruitment of cellular repair proteins to HPV replication centers would facilitate viral replication but could leave chromosomal DNA unrepaired. Our present work shows how HPV delays the repair of ICLs and attenuates the FA DNA repair pathway. Mislocalization of FancD2 observed in our study may represent a fruitless attempt to bring the FancD2 repair protein to non-existing viral replication centers. This would attenuate ICL repair regardless of the presence or absence of the viral genome because FancD2 helps in the recruitment of downstream FA repair

proteins, including Rad51 in nuclear foci at the site of DNA damage. This is supported by our data demonstrating that mislocalized FancD2 in E6 cells causes a reduction in Rad51 recruitment to DSBs (Fig 4G–4H).

FancD2 monoubiquitination is necessary for ICL repair, but, by itself, is not sufficient for an efficient FA pathway. In other words, having more monoubiquitinated FancD2 within a cell does not necessarily improve ICL repair. This is exemplified by studies demonstrating that USP1-mediated FancD2 de-ubiquitination is required for both FancD2 foci formation and ICL sensitivity [10, 13] and for a functional FA pathway [7, 12, 45]. HPV E6 caused the delayed de-ubiquitination of FancD2, impairing ICL repair (Fig 5). HPV E6 cells showed increased phosphorylated S565 FancI and persistently activated ATR/CHK-1, which may, in part, cause delayed FancD2 de-ubiquitination in these cells. The delayed de-ubiquitination pattern observed in E6 expressing cells may be also due to a block at the step of release of FancD2 from chromatin which hinders USP1 deubiquitination activity.

ATR/CHK1 signaling is a key step in activating the FA pathway [5]. ATR is activated when the replication fork encounters DNA damage. ATR then phosphorylates several substrates, including FancD2 and FancI as well as members of the FA core complex. ATR-mediated FancI phosphorylation at Serine 556 (called ubiquitination-independent phosphorylation) occurs predominantly upstream of, and promotes, the monoubiquitination of FancD2/ FancI [7, 63]. On the other hand, FancI Serine 565 phosphorylation (called ubiquitination-linked phosphorylation) occurs downstream of Ub-FancD2/I and inhibits FancD2 de-ubiquitination [7]. Augmented ATR activity in E6 expressing cells resulted in increased phosphorylation of FancI at both sites S556 and S565. Increased p-S556 FancI promotes the monoubiquitination of FancD2, but at the same time elevated p-S565 FancI inhibits de-ubiquitination.

Together, we provide a mechanistic framework for HR-HPV oncogenes disruption of the FA DNA repair pathway (S11 Fig). This study advances our understanding of HPV tumorigenesis as well as tumor sensitivity to cisplatin during chemotherapy. Our study suggests a general model for the progression of HPV associated cancers. Over the multi-decade course of HPV-induced tumorigenesis, persistent expression of HPV oncogenes impairs the FA pathway. This leads to cells with destabilized genomes, allowing for rapid tumor progression. Previous studies are in support of the model that dysregulated FA pathway contributes to the development of cancers in patients without FA [64–66] and with FA [67, 68]. An extremely high incidence of cancer in FA patients [69] further suggest that the inactivation of FA pathway results in tumor progression.

Our work also has important therapeutic implications. Because continued expression of HPV oncogenes is required for cancer development, most HPV-associated tumors likely have defective FA pathway. These defects result in cisplatin hypersensitivity and demonstrate the mechanisms underlying the therapeutic efficacy of cisplatin in HPV-associated cancers. This also explains the reason underlying the better response rates of HPV+ oropharyngeal cancers than HPV negative head and neck cancers to cisplatin treatment. We believe that tumors that are cisplatin resistant, may have adapted other unexplored mechanisms to escape these defects. One possibility is that some cells with an intact FA pathway are positively selected during cancer progression, resulting in the growth of a cisplatin-resistant tumor.

Materials and methods

Ethics statement

The use of deidentified neonatal human foreskins for the study was approved by the Institutional Review Board at the Swedish Medical Center (Seattle, WA). Tissues from newborn circumcisions were collected from Swedish First Hill Birth Center, Seattle, WA.

Cell culture, transduction, and treatment

Primary human foreskin keratinocytes (HFKs) were generated from deidentified neonatal human foreskins and grown in EpiLife Medium supplemented with 60 μM calcium chloride (ThermoFisher Scientific, MEPI500CA) and human keratinocyte growth supplement (ThermoFisher Scientific, S0015). HFKs derived from multiple donors were used to repeat the results. U2OS DR-GFP cells (a gift from Maria Jasin) were grown in DMEM supplemented with 10% FBS. U2OS DR-GFP cells contain a single integrated copy of the DR-GFP cassette [70].

Retroviruses were produced in 293T cells (Thermo Fisher Scientific) using plasmid constructs (LTR/VSV-G, CMV/tat, pJK3 and pLXSN vector- empty, E6, E7 or E6E7, or E6 8S/9A/10T mutant) and TransIT-293 transfection reagent (Mirus Bio) according to manufacturer's protocol. Following retroviral transduction and G418 selection (50ug/ml) in HFKs or U2OS-DR cells, the expression of HPV16 oncogenes E6 and E7 was confirmed by qRT-PCR of 16 E6 and E7 and immunoblot to p53 and pRB (well-characterized cellular targets). The expression of p53 in HFKs was suppressed using transduction-ready p53 shRNA lentiviral particles (Santa Cruz Biotechnology, sc-29435-V). HFKs were transduced with lentiviral stock in media containing 10ug/ml polybrene. Following 48 hr of transduction, stably transduced cells were selected in 0.5 ug/ml puromycin and the efficiency of knockdown was monitored using immunoblot to p53.

Cells were treated with cisplatin (Selleck Chemicals, S1166), Mitomycin C (MMC) (Sigma, M4287), Nutlin-3a (Selleck Chemicals, S8059), VE-821 (Selleck Chemicals, S8007), cycloheximide (Millipore 239763), Ionizing radiation (IR) (GammaCell Cesium Irradiator -1000) or UVB (two FS20t12/UVB bulbs, Solarc Systems, Inc.). Cisplatin was dissolved at the stock of 1.5mM in 0.9% NaCl (sterile), Nutlin-3a and VE-821 at the stock of 10mM in DMSO, cycloheximide at the stock of 50mg/ml in DMSO, aliquoted and kept at -20˚ C protected from light.

Antibodies

Primary antibodies against p53 (Cell Signaling Technology, 9282), pRb (BD Pharmingen, 554136), FancD2 (Santa Cruz Biotechnology, FI17, sc-20022 or Abcam, ab2187), FancI (Santa Cruz Biotechnology, A-7, sc-271316), Phospho-Ser556 FancI and Phospho-Ser565-FancI (gifts from Ronald Cheung, Toshiyasu Taniguchi lab), pH2AX (Millipore, 05–636), Rad51 (Cosmo Bio Co. Ltd, 70–001), Palb2 (Bethyl Laboratories, A301-246A), Palb2 (a gift from Bing Xia, Rutgers Cancer Institute), Phospho-ATR (Ser428) (Cell Signaling Technology, 2853), Phospho-Chk1 (Ser345) (133D3) (Cell Signaling Technology, 2348), ATR (Cell Signaling Technology, 2790), CHK1 (2G1D5, Cell Signaling Technology, 2360), PCNA (PC10) (Cell Signaling Technology, 2586), Ubiquityl-PCNA (Lys164) (Cell Signaling Technology, 13439), UHRF1 (Santa Cruz Biotechnology, H-8, sc-373750), USP1 (C-term; a gift from Tony Huang, NYU School of Medicine), Cyclin A (in-house, Clurman lab), Beta actin (GeneTex, GTX110564 or Cell Signaling Technology, 5125), Vinculin (Sigma, V9131), and Histone H3 (Abcam, ab1791), GAPDH (14C10, Cell Signaling Technology, 2118)were used. Secondary antibodies were conjugated with horse radish peroxidase (mouse or rabbit, Cell Signaling Technology) or appropriate Alexa Fluor (Molecular Probes) were used.

Cell extraction, fractionation, and immunoblotting

Whole cell lysates were prepared by directly lysing cell pellets in SDS sample buffer (0.05 M Tris-HCl, (pH 6.8), 2% SDS, 6% β-mercaptoethanol) and boiling for 5 min. Cell fractionation was performed to obtain soluble and chromatin-bound fractions, as described [71]. Briefly, cell pellets were re-suspended in CSK + 0.1% Triton-X buffer (10mM PIPES, pH = 6.8,

100mM NaCl, 1mM EGTA, 1mM EDTA, 300mM Sucrose, 1.5mM MgCl2, 0.1% Triton-X-100 and protease inhibitors) and incubated on ice for 5 mins. After centrifugation (1500g for 5 min), the supernatant was collected and stored (soluble fraction). Pellet (Chromatin-bound fraction) was washed twice in CSK buffer and then resuspended in SDS sample buffer and boiled for 5 min. Samples were stored at -20 ˚C until quantification and immunoblotting. Proteins were quantified using Bradford protein assay (Bio-rad) and processed using NuPAGE LDS sample buffer (ThermoFisher Scientific) for loading equal amounts (15ug) onto the gels. SDS-PAGE electrophoresis was done using NuPAGE 3–8% Tris-acetate or 4–12% Tris-glycine gels (ThermoFisher Scientific) and proteins were transferred to Immobilon-P PVDF membranes (Millipore). Primary antibodies were diluted in blocking buffer (4% milk in TBS-Tween 20) or in 3% BSA in TBST for phosphorylated proteins and incubated overnight at 4 ˚C. Horseradish peroxidase (HRP)-conjugated anti-mouse or anti-rabbit secondary antibodies were used. Blots were developed using Clarity Western ECL substrate (Bio-Rad) and images were acquired using ChemiDoc MP Imaging System (Bio-Rad) and processed using Image Lab Software (Bio-Rad). Band quantification was performed using ImageJ, normalizing with a loading control.

RT-PCR

qRT-PCR was conducted to evaluate the expression of HPV16 E6, E7, and GADPH genes, as described previously [3]. To evaluate the expression of FancD2 mRNA, two sets of primers were designed to amplify the longer FancD2 isoform from transcript sequence NM_033084.4. The first primer set adapted from Jaber et al. [46] was Forward 5'-AGACTGTCAAAATCTGAGGATAAAGAGA-3' and Reverse 5'-TGGTTGCTTCCTGGTTTTGG-3'; and next set was designed as Forward 5'-CATGGCTGTTCGAGACTTC-3' and Reverse 5'-CACAAAGAGACGCCCATAC-3'. Other primers used were FancI: Forward 5'-TGGCGGAGTTCTGTGATATGAG-3' and Reverse 5'-CAGAGCAGGGGGAACCTTTG-3', Palb2: Forward 5'- GCTCTTTTCGTTCTGTCGCC-3' and Reverse 5' TCTCCTTTAACTTTTCCTTCTCCTC-3', and UHRF1: Forward 5'- TTCCCGCCGACACCAT-3' and Reverse 5' TCCTCCATCTGTTTGCCCC-3'.

Cycloheximide chase assay

To compare protein stability or turnover, cells were treated with 50 ug/ml cycloheximide (CHX), an inhibitor of protein biosynthesis and the protein levels were monitored over a 24 hr period. Cell lysates were collected at indicated time points followed by immunoblotting for FancD2, FancI, UHRF1 and Palb2. GAPDH was selected as a loading control whose level did not change following the addition of cycloheximide till a 24 hr period.

Cisplatin cell survival assay

Cell survival over a range of cisplatin concentrations was measured using a crystal violet absorbance-based assay [72]. Briefly, cells were seeded on 24-well plate overnight and treated with cisplatin at indicated doses for 3 days. Cells were then washed once with PBS and fixed for 10 min at room temperature in 10% methanol and 10% acetic acid. Adherent cells were stained with 0.5% crystal violet in methanol. Plates were rinsed in water and allowed to dry completely. The adsorbed dye was re-solubilized with methanol containing 0.1% (wt/vol) SDS by gentle agitation for 2 hr at room temperature. Dye solution (200 μl) was transferred to 96-well plates and diluted (1:2) in methanol. Absorbance was measured at 595 nm. Cell survival was calculated by normalizing the absorbance relative to untreated controls.

siRNA transfection

siRNAs were transfected at a final concentration of 20nM in 6-well or 10 cm plates using Lipofectamine RNAiMAX (Invitrogen), following the manufacturer's Reverse Transfection protocol. I-SceI colocalization and crystal violet assays were conducted, respectively 24 and 48 hr after siRNA transfection. The following siRNAs were used: si-FancD2: 5'- AACAGCCAUGGAUACACUUGA-3'; si-Palb2 (Santa Cruz Biotechnology, sc-93396), siATR (Santa Cruz Biotechnology, sc-29763), siPCNA (Santa Cruz Biotechnology, sc-29440), siUHRF1 (Santa Cruz Biotechnology, sc-7680) and siRNA Universal Negative Control#1 (Sigma, SIC001). Knockdown was confirmed by immunoblotting.

Immunofluorescence microscopy

HFKs and U2OS DR-GFP cells (transduced with LXSN, 16 E6, 16 E7 and 16 E6E7) were grown in chamber slides overnight. Cells were either left untreated or treated with cisplatin or transfected with I-SceI expression vector (Addgene, 26477). Cells were then washed with 1X PBS and fixed and co-permeabilized using 2% paraformaldehyde and 0.5% Triton-X in PBS for 30 mins. After washing, cells were blocked with 3% BSA and 0.1% Tween20 in PBS for 1 hr. Cells were then subsequently incubated with appropriate primary antibodies (indicated in the text) in a moist chamber at 4˚ C overnight. The following day, cells were washed 3 times with 1X PBST (1X PBS + 0.1% Tween20) for 5 min each and then incubated for 1 hr at room temperature with Alexa Fluor secondary antibodies in dark. Primary and secondary antibodies were diluted in blocking buffer. Following secondary antibody incubation, cells were washed and mounted using coverslip in ProLong Diamond Antifade Mountant with DAPI (Molecular Probes). Cells were then visualized using a DeltaVision Elite confocal microscope (Applied Precision). The images were deconvolved using the Deltavision SoftWoRx program and were analyzed using ImageJ. Each experiment was repeated at least 3 times independently.

I-SceI colocalization assay

I-SceI colocalization assay in U2OS-DR cells (transduced with LXSN, E6, E7 or E6E7) were performed as described previously [3]. Briefly, cells were transfected with I-SceI expression vector using TransIT-LT1 reagent (Mirus) and were stained for pH2AX and the indicated protein. In the case of gene knockdown experiments, reverse siRNA transfection was done a day before transfecting I-SceI plasmid. A single large pH2AX foci created by I-SceI expression was inspected for its colocalization with indicated repair protein.

Alkaline comet assay

Repair of interstrand crosslinks was assessed by an alkaline comet assay [32–34] using Trevigen's CometAssay (4250-050-K), following the manufacturer's protocol with some modifications. Cells were treated with 1.5 uM cisplatin for 2 hr. At the end of treatment, cells were washed with PBS and incubated in fresh medium for the required post-incubation time or harvested immediately (time 0 h). To process all the samples concurrently and to eliminate assay variability, cells were harvested and cryopreserved in media containing 10% DMSO and 50% FBS, prior to performing comet assay. Immediately before analysis, cells were thawed in ice-cold DPBS and irradiated with 12 Gy gamma irradiation (using GammaCell Irradiator GC-1000) to introduce a fixed number of random DNA strand breaks and processed according to Trevigen's alkaline Comet assay procedures. Briefly, irradiated or unirradiated cells were immediately plated in low melting agarose on slides. After hardening of the agarose gel, cells were lysed and subjected to alkaline electrophoresis for 30 min at 4˚ C. After air-drying, DNA

was visualized using SYBR Gold and images were captured using TissueFAXS machine using FITC filter. Images were analyzed using OpenComet Plugin tool in NIH ImageJ [73]. Default background correction was used. The output images resulting from the automatic analysis were manually reviewed to eliminate outliers and select uniform comets. Updated tail moment values (Mean ± SE from >350 comets) were then used to calculate % ICL remaining.

The degree of DNA ICLs present in the cisplatin-treated sample was calculated by comparing the tail moment of cisplatin-treated and irradiated (Cp.IR) samples with irradiated untreated (IR) samples and unirradiated untreated (Ø) control samples. The level of ICL is proportional to the decrease in the tail moment in the irradiated cisplatin treated sample compared to the irradiated untreated control. To quantify ICL repair (or the percentage of ICL remaining), we employed the following formula:

$$\%\ \text{Decrease in tail moment(or ICL remaining)} = [1 - (\text{Cp.IR} - \oslash)/(\text{IR} - \oslash)]\ \text{x}\ 100$$

where Cp.IR = mean tail moment of cisplatin-treated and irradiated cells; Ø = mean tail moment of untreated and unirradiated cells, and IR = mean tail moment of irradiated and untreated cells.

The data were expressed as the percentage of ICLs that remained at a specific time point where 0 hr was normalized to 100%.

Cell-cycle synchronization and analysis

Cells were synchronized at G1/S phase boundary by double-thymidine block and cell pellets were harvested for immunoblotting and flow cytometry analysis as described previously [4, 74], with some modifications. Briefly, HFK cells were treated with 2 mM thymidine (Sigma-Aldrich) in EpiLife media without growth supplements for 16 hours. Cells were then washed twice with PBS and released/grown in thymidine-free complete EpiLife media for 9 hours. Thereafter, cells were treated again with 2 mM thymidine in growth supplement-free EpiLife media for another 16 hours. Cells were washed twice with PBS and then released in complete media and harvested every 3 hours after release. Synchronized cells were analyzed at different time points by immunoblotting and analyzing DNA content by DAPI staining. Approximately 10,000 cells were analyzed using flow cytometry (BD FACS-Canto II), and flow histograms were generated using FlowJo software.

Statistics

All statistical analyses were done using Student's t-test (Unpaired two-tailed) in GraphPad Prism. P value < 0.05 was considered significant. Statistical significance at $P < 0.05$, $P < 0.01$, $P<0.001$ and $P < 0.0001$ are indicated as *, **, ***, **** respectively.

Supporting information

S1 Fig. The Fanconi anemia repair pathway. Endogenous (aldehydes) and exogenous (cisplatin) agents cause interstrand crosslink lesions (ICL). The stalled replication fork at ICL site activates ATR signaling and recruits the FA core complex (FancA, B, C, E, F, G, L, and M). FancL with the help of FancT catalyze the monoubiquitination of the FancD2-FancI (ID) complex. Monoubiquinated ID complex helps in the recruitment of downstream repair proteins, including FancD1/BRCA2, FancS/BRCA1, FancN/Palb2, FancR/Rad51, and FancJ/BRIP1. These proteins crosstalk with other DNA repair pathways such as the nucleotide excision, homologous recombination and translesion synthesis to repair ICLs. ATR-mediated FancI phosphorylation at Serine 556 occurs upstream of, and promotes, the monoubiquitination of ID complex, whereas phosphorylation at Serine 565 occurs downstream of

monoubiquitination and inhibit FancD2 deubiquitination.
(TIF)

S2 Fig. E6 expressing cells showed high Ub-FANCD2 & -FANCI both at baseline and after cisplatin/ MMC treatment. (A-B) Confirmation of HPV16 E6 and E7 expression by qRT-PCR (A) and immunoblot of p53 and pRb in HFK cells (B). Immunoblot showing FancD2/ FancI expression and monoubiquitination status in LXSN and E6 cells which (C) were either untreated or treated with 60ng/ml mitomycin C for 24 hr, and (D) were exposed to 10 mJ/cm2 UVB and incubated for indicated time points. (E) Immunoblot of transduced HFK cells harvested following different lengths of cisplatin treatment. Ub refers to the monoubiquitinated forms of FancD2 and FancI, and non-Ub refers to the non-ubiquitinated forms. Asterisks (*) indicate a non-specific band.
(TIF)

S3 Fig. Determination of transcription and protein turnover rate of FancD2, FancI and UHRF1. (A) Relative mRNA expression of FanCD2, FancI and UHRF1 in HFK cells. (B-C) LXSN and E6 expressing cells were treated with 50ug/ml cycloheximide for the indicated times to determine protein turnover rate. Immunoblots (B) from a representative experiment are shown. (C) Intensities of protein bands were measured and normalized to those of GAPDH and were quantified relative to 0 hr from 2 independent experiments.
(TIF)

S4 Fig. ATR/p-S556 FancI, but not UHRF1 and PCNA help in increasing Ub-FancD2. (A-C) Immunoblots showing the effective knockdown of ATR, UHRF1 and PCNA. (D-F) Immunoblots showing FancD2 mono or de-ubiquitination status in the cells which were transfected with siControl or respective siRNAs and were either untreated or treated with 1.5 uM cisplatin 24 hr. Levels of total FancD2 (Ub + Non-Ub) and total FancI normalized to vinculin, and ratios of phosphorylated FancI to total FancI are indicated beneath the corresponding lanes in S4D Fig.
(TIF)

S5 Fig. Rad51 colocalization with FancD2 in HFK-LXSN cells. (A) Schematic of I-SceI colocalization assay. The DR-GFP reporter cassette (integrated into U2OS genome) consists of two copies of nonfunctional GFP gene. The first copy is inactive due to the presence of a stop codon within the I-SceI cleavage site, while the second copy (iGFP) is truncated at both ends. Exogenous expression of I-SceI in U2OS cells with one integrated copy of the I-SceI recognition site produces a single persistent DSB. Recruitment of repair protein (green) to this enlarged pH2AX focus (red) can be visualized by IF. (B) HFK cells (transduced with LXSN) were treated with cisplatin (3 uM for 24 hr) and immunostained with FancD2 (red), Rad51 (green) and DAPI (blue). Representative images are shown.
(TIF)

S6 Fig. ATR/CHK signaling contributes to the delayed FancD2 de-ubiquitination in E6 expressing cells. (A-B) Cells were exposed to 10 mJ/cm2 UVB and incubated for indicated time points. (A) Cells were stained with DAPI and p-ATR antibody. (B) Cells were harvested at the indicated time points, and lysates were immunoblotted with antibodies to p-CHK1 and actin. (C-D) Cells were treated with 1.5uM cisplatin for 24 hr. After cisplatin withdrawal, cells were either grown in normal media (no drug) or treated with 10uM VE821 (ATR inhibitor) for indicated time points. Immunoblots of LXSN and E6 expressing cells. FancD2 Ub: non-Ub ratio are indicated beneath the corresponding lanes. pCHK1 (Serine 345) western blotting

confirmed ATR inhibition by VE821.
(TIF)

S7 Fig. P53 knockdown does not change total and monoubiquitinated levels of FancD2. (A) Immunoblot showing p53 knockdown in or p53 shRNA cells compared to LXSN control. (B) Immunoblot showing FancD2 expression and monoubiquitination status in HFK LXSN and p53 knockdown cells which were either untreated or treated with 1.5 uM cisplatin for 24 hr.
(TIF)

S8 Fig. Delayed FancD2 deubiquitination in E6 cells is dependent on p53 degradation. (A) Immunoblots showing FancD2 mono- and deubiquitination status in HFKs which were treated with 1.5 uM cisplatin (upper panel) or 0.75uM cisplatin (lower panel) for 24 hr and allowed to repair, following cisplatin withdrawal. Initial experiments treating mutE6 cells with 1.5uM cisplatin and subsequent withdrawal did not give a clear idea (the deubiquitination pattern was more likely in between LXSN and E6). Therefore, less concentrated cisplatin (0.75uM) was used (Fig 7E). However, in case of LXSN cells, 0.75uM cisplatin treatment for 24hr was not enough to induce predominant mono-ubiquitinated FancD2 fraction. (B) Immunoblots showing FancD2 mono- and deubiquitination status in LXSN and p53 knockdown cells following UVB exposure (upper panel) and cisplatin withdrawal (lower panel). (C) Immunoblot for p-ATR, pCHK1, FancD2 and p-FancI-S565 in E6 and mutant E6 cells following cisplatin withdrawal for 18 and 24 hrs. Vinculin acts as a loading control.
(TIF)

S9 Fig. E6-mediated decreased Palb2 level is due to increased Palb2 turnover but independent of p53 degradation. Immunoblot showing Palb2 expression in (A) HFKs transduced with LXSN or E6/E7 untreated or 2hrs after UV exposure (B) in HFKs transduced with LXSN, E6 or mutant E6. Vinculin serves as a loading control. (C) Relative mRNA expression of Palb2 in HFKs (D) Cells were treated with 50ug/ml cycloheximide for the indicated times to determine protein turnover rate. Immunoblots (top) from a representative experiment are shown. Densitometric analysis from 2 independent experiments (bottom). Bands were normalized with GAPDH and were relative to 0 hr.
(TIF)

S10 Fig. E6 does not affect the colocalization of Palb2 to DSBs and Rad51 recruitment defect associated with E6 is not due to Palb2. (A) U20S-DR cells transduced with LXSN, or E6/E7 were transfected with I-SceI expression plasmid to induce DSB. Representative images showing cells with a single large pH2AX focus (red), were inspected for the colocalization with Palb2 (green), upper panel. Quantification of the frequency of colocalization of Palb2 with pH2AX focus (right panel). Data represent mean ± SEM and was based on observations from $\geq$ 25 cells from 3 independent experiments. (B) U2OS-DR cells were transfected first with the siControl or siPalb2 and then with I-SceI plasmid and were stained with Rad51 and pH2AX antibodies. Representative images showing U20S E7 cells stained with pH2AX (red), Rad51 (green), and DAPI, upper panel. Graph showing %Rad51 colocalization in siPalb2 cells compared to similarly transfected cells (right panel). * and ** indicate significance respectively at $p<0.05$ and $p<0.01$ (compared to siControl cells).
(TIF)

S11 Fig. HPV oncogenes impair the Fanconi anemia repair pathway. E6 or E7 causes persistence of DNA interstrand crosslinks and increases cisplatin sensitivity. HPV oncogenes though promote the initiation of the FA pathway by increasing FancD2 monoubiquitination and foci

formation (Figs 3 and 4), they attenuate the completion of the pathway by multiple mechanisms. First, E6/E7 reduces the recruitment of FancD2 to double strand breaks (DSBs). We hypothesize that DNA repair proteins including FancD2 localize to single stranded DNA breaks (SSB) that could occur at replication forks. Second, E6 causes mislocalization of Rad51 from DSBs because FancD2 which helps in Rad51 recruitment itself is mislocalized (Fig 4). Third, E6 reduces Palb2 level and foci formation, which is due to increased Palb2 protein turnover (Fig 8 and S9 Fig). Lastly, E6 causes delayed FancD2 deubiquitination, impairing the functional FA pathway. Delayed FancD2 de-ubiquitination is due to persistently activated ATR/CHK-1/pS565 FancI signaling. and the increased chromatin retention of FancD2 hindering USP1 de-ubiquitinating activity (Fig 5).
(TIF)

Acknowledgments

We acknowledge Ronald Cheung from the Taniguchi lab for helpful guidance, advice, and discussions. Ahmed Diab from Clurman lab was helpful in designing experiments and having helpful discussions. We thank Bing Xia (Rutgers Cancer Institute) for Palb2 antibody and Tony T. Huang (NYU School of Medicine) for the USP1 antibody. We acknowledge current and former members of Galloway lab for assistance and suggestions. We are grateful to Ann Roman for critical reading of this manuscript.

We thank Julio Vazquez Lopez and David McDonald of the FHCRC Scientific Imaging Facility for their help in immunofluorescence imaging. Staff of the FHCRC Flow Cytometry Facility were very helpful with FACS analysis.

Author Contributions

Conceptualization: Sujita Khanal, Denise A. Galloway.

Data curation: Sujita Khanal.

Formal analysis: Sujita Khanal.

Funding acquisition: Denise A. Galloway.

Investigation: Sujita Khanal, Denise A. Galloway.

Project administration: Denise A. Galloway.

Software: Denise A. Galloway.

Supervision: Denise A. Galloway.

Writing – original draft: Sujita Khanal.

Writing – review & editing: Denise A. Galloway.

References

1. Moody C.A. and Laimins L.A., Human papillomavirus oncoproteins: pathways to transformation. Nature Reviews Cancer, 2010. 10(8): p. 550. https://doi.org/10.1038/nrc2886 PMID: 20592731
2. CDC, HPV-Associated Cancer Statistics. 2017, Centers for Disease Control and Prevention (CDC): https://www.cdc.gov/cancer/hpv/statistics/index.htm.
3. Wallace N.A., et al., High-Risk Alphapapillomavirus Oncogenes Impair the Homologous Recombination Pathway. J Virol, 2017. 91(20).
4. Taniguchi T., et al., Convergence of the fanconi anemia and ataxia telangiectasia signaling pathways. Cell, 2002. 109(4): p. 459–72. PMID: 12086603

5. Nalepa G. and Clapp D.W., Fanconi anaemia and cancer: an intricate relationship. Nature Reviews Cancer, 2018.
6. Fanconi Anemia Mutation Database, Leiden Open Source Variation Database (LOVD v.3.0). 2018, The Rockefeller University: http://www2.rockefeller.edu/fanconi/.
7. Cheung R.S., et al., Ubiquitination-Linked Phosphorylation of the FANCI S/TQ Cluster Contributes to Activation of the Fanconi Anemia I/D2 Complex. Cell Rep, 2017. 19(12): p. 2432–2440. https://doi.org/10.1016/j.celrep.2017.05.081 PMID: 28636932
8. Ceccaldi R., Sarangi P., and D'Andrea A.D., The Fanconi anaemia pathway: new players and new functions. Nat Rev Mol Cell Biol, 2016. 17(6): p. 337–49. https://doi.org/10.1038/nrm.2016.48 PMID: 27145721
9. Andreassen P.R., D'Andrea A.D., and Taniguchi T., ATR couples FANCD2 monoubiquitination to the DNA-damage response. Genes Dev, 2004. 18(16): p. 1958–63. https://doi.org/10.1101/gad.1196104 PMID: 15314022
10. Oestergaard V.H., et al., Deubiquitination of FANCD2 is required for DNA crosslink repair. Mol Cell, 2007. 28(5): p. 798–809. https://doi.org/10.1016/j.molcel.2007.09.020 PMID: 18082605
11. Kim J.M., et al., Inactivation of murine Usp1 results in genomic instability and a Fanconi anemia phenotype. Dev Cell, 2009. 16(2): p. 314–20. https://doi.org/10.1016/j.devcel.2009.01.001 PMID: 19217432
12. Nijman S.M., et al., The deubiquitinating enzyme USP1 regulates the Fanconi anemia pathway. Mol Cell, 2005. 17(3): p. 331–9. https://doi.org/10.1016/j.molcel.2005.01.008 PMID: 15694335
13. Liang Q., et al., A selective USP1-UAF1 inhibitor links deubiquitination to DNA damage responses. Nat Chem Biol, 2014. 10(4): p. 298–304. https://doi.org/10.1038/nchembio.1455 PMID: 24531842
14. Park E., et al., Inactivation of Uaf1 causes defective homologous recombination and early embryonic lethality in mice. Molecular and cellular biology, 2013. 33(22): p. 4360–4370. https://doi.org/10.1128/MCB.00870-13 PMID: 24001775
15. Hoskins E.E., et al., Fanconi anemia deficiency stimulates HPV-associated hyperplastic growth in organotypic epithelial raft culture. Oncogene, 2009. 28(5): p. 674–85. https://doi.org/10.1038/onc.2008.416 PMID: 19015634
16. Hoskins E.E., et al., The fanconi anemia pathway limits human papillomavirus replication. J Virol, 2012. 86(15): p. 8131–8. https://doi.org/10.1128/JVI.00408-12 PMID: 22623785
17. Park J.W., et al., Deficiencies in the Fanconi anemia DNA damage response pathway increase sensitivity to HPV-associated head and neck cancer. Cancer Res, 2010. 70(23): p. 9959–68. https://doi.org/10.1158/0008-5472.CAN-10-1291 PMID: 20935219
18. Park J.W., Shin M.-K., and Lambert P.F., High incidence of female reproductive tract cancers in FA-deficient HPV16-transgenic mice correlates with E7's induction of DNA damage response, an activity mediated by E7's inactivation of pocket proteins. Oncogene, 2014. 33(26): p. 3383. https://doi.org/10.1038/onc.2013.327 PMID: 24013229
19. Kutler D.I., et al., A 20-year perspective on the International Fanconi Anemia Registry (IFAR). Blood, 2003. 101(4): p. 1249–56. https://doi.org/10.1182/blood-2002-07-2170 PMID: 12393516
20. van Zeeburg H.J., et al., Clinical and molecular characteristics of squamous cell carcinomas from Fanconi anemia patients. J Natl Cancer Inst, 2008. 100(22): p. 1649–53. https://doi.org/10.1093/jnci/djn366 PMID: 19001603
21. Kutler D.I., et al., Human papillomavirus DNA and p53 polymorphisms in squamous cell carcinomas from Fanconi anemia patients. J Natl Cancer Inst, 2003. 95(22): p. 1718–21. PMID: 14625263
22. de Araujo M.R., et al., High prevalence of oral human papillomavirus infection in Fanconi's anemia patients. Oral Dis, 2011. 17(6): p. 572–6. https://doi.org/10.1111/j.1601-0825.2011.01803.x PMID: 21332606
23. Alter B.P., et al., Squamous cell carcinomas in patients with Fanconi anemia and dyskeratosis congenita: a search for human papillomavirus. Int J Cancer, 2013. 133(6): p. 1513–5. https://doi.org/10.1002/ijc.28157 PMID: 23558727
24. Ziemann F., et al., Increased sensitivity of HPV-positive head and neck cancer cell lines to x-irradiation +/- Cisplatin due to decreased expression of E6 and E7 oncoproteins and enhanced apoptosis. Am J Cancer Res, 2015. 5(3): p. 1017–31. PMID: 26045983
25. Hoskins E.E., et al., Coordinate regulation of Fanconi anemia gene expression occurs through the Rb/E2F pathway. Oncogene, 2008. 27(35): p. 4798–808. https://doi.org/10.1038/onc.2008.121 PMID: 18438432
26. Spardy N., et al., HPV-16 E7 reveals a link between DNA replication stress, fanconi anemia D2 protein, and alternative lengthening of telomere-associated promyelocytic leukemia bodies. Cancer Res, 2008. 68(23): p. 9954–63. https://doi.org/10.1158/0008-5472.CAN-08-0224 PMID: 19047177

27. Spardy N., et al., The human papillomavirus type 16 E7 oncoprotein activates the Fanconi anemia (FA) pathway and causes accelerated chromosomal instability in FA cells. J Virol, 2007. 81(23): p. 13265–70. https://doi.org/10.1128/JVI.01121-07 PMID: 17898070

28. Wallace N.A., et al., HPV 5 and 8 E6 abrogate ATR activity resulting in increased persistence of UVB induced DNA damage. PLoS Pathog, 2012. 8(7): p. e1002807. https://doi.org/10.1371/journal.ppat.1002807 PMID: 22807682

29. Zhang Y., et al., BRCA1 interaction with human papillomavirus oncoproteins. Journal of Biological Chemistry, 2005. 280(39): p. 33165–33177. https://doi.org/10.1074/jbc.M505124200 PMID: 15983032

30. Reinson T., et al., Engagement of the ATR-dependent DNA damage response at the human papillomavirus 18 replication centers during the initial amplification. Journal of virology, 2013. 87(2): p. 951–964. https://doi.org/10.1128/JVI.01943-12 PMID: 23135710

31. Spriggs C.C. and Laimins L.A., FANCD2 Binds Human Papillomavirus Genomes and Associates with a Distinct Set of DNA Repair Proteins to Regulate Viral Replication. MBio, 2017. 8(1).

32. Wu J.H. and Jones N.J., Assessment of DNA interstrand crosslinks using the modified alkaline comet assay, in *Genetic Toxicology*. 2012, Springer. p. 165–181.

33. Hartley J.M., et al., Measurement of DNA cross-linking in patients on ifosfamide therapy using the single cell gel electrophoresis (comet) assay. Clinical Cancer Research, 1999. 5(3): p. 507–512. PMID: 10100700

34. Olive P.L. and Banáth J.P., Kinetics of H2AX phosphorylation after exposure to cisplatin. Cytometry Part B: Clinical Cytometry, 2009. 76(2): p. 79–90.

35. Riddell I.A. and Lippard S.J., Cisplatin and Oxaliplatin: Our Current Understanding of Their Actions. Metallo-Drugs: Development and Action of Anticancer Agents: Development and Action of Anticancer Agents, 2018. 18: p. 1.

36. Howlett N.G., et al., Functional interaction between the Fanconi Anemia D2 protein and proliferating cell nuclear antigen (PCNA) via a conserved putative PCNA interaction motif. J Biol Chem, 2009. 284(42): p. 28935–42. https://doi.org/10.1074/jbc.M109.016352 PMID: 19704162

37. Geng L., Huntoon C.J., and Karnitz L.M., RAD18-mediated ubiquitination of PCNA activates the Fanconi anemia DNA repair network. J Cell Biol, 2010. 191(2): p. 249–57. https://doi.org/10.1083/jcb.201005101 PMID: 20937699

38. Liang C.C., et al., UHRF1 is a sensor for DNA interstrand crosslinks and recruits FANCD2 to initiate the Fanconi anemia pathway. Cell Rep, 2015. 10(12): p. 1947–56. https://doi.org/10.1016/j.celrep.2015.02.053 PMID: 25801034

39. Tian Y., et al., UHRF1 contributes to DNA damage repair as a lesion recognition factor and nuclease scaffold. Cell Rep, 2015. 10(12): p. 1957–66. https://doi.org/10.1016/j.celrep.2015.03.038 PMID: 25818288

40. Williams S.A., et al., The E3 ubiquitin ligase RAD18 regulates ubiquitylation and chromatin loading of FANCD2 and FANCI. Blood, 2011. 117(19): p. 5078–87. https://doi.org/10.1182/blood-2010-10-311761 PMID: 21355096

41. Pierce A.J., et al., XRCC3 promotes homology-directed repair of DNA damage in mammalian cells. Genes & development, 1999. 13(20): p. 2633–2638.

42. Taniguchi T., et al., S-phase–specific interaction of the Fanconi anemia protein, FANCD2, with BRCA1 and RAD51. Blood, 2002. 100(7): p. 2414–2420. https://doi.org/10.1182/blood-2002-01-0278 PMID: 12239151

43. Sato K., et al., FANCI-FANCD2 stabilizes the RAD51-DNA complex by binding RAD51 and protects the 5′-DNA end. Nucleic acids research, 2016. 44(22): p. 10758–10771. PMID: 27694619

44. Thompson E.L., et al., FANCI and FANCD2 have common as well as independent functions during the cellular replication stress response. Nucleic acids research, 2017. 45(20): p. 11837–11857. https://doi.org/10.1093/nar/gkx847 PMID: 29059323

45. van Twest S., et al., Mechanism of Ubiquitination and Deubiquitination in the Fanconi Anemia Pathway. Mol Cell, 2017. 65(2): p. 247–259. https://doi.org/10.1016/j.molcel.2016.11.005 PMID: 27986371

46. Jaber S., et al., p53 downregulates the Fanconi anaemia DNA repair pathway. Nature communications, 2016. 7: p. 11091. https://doi.org/10.1038/ncomms11091 PMID: 27033104

47. Foster S.A., et al., The ability of human papillomavirus E6 proteins to target p53 for degradation in vivo correlates with their ability to abrogate actinomycin D-induced growth arrest. Journal of virology, 1994. 68(9): p. 5698–5705. PMID: 8057451

48. Kiyono T., et al., Both Rb/p16 INK4a inactivation and telomerase activity are required to immortalize human epithelial cells. Nature, 1998. 396(6706): p. 84. https://doi.org/10.1038/23962 PMID: 9817205

49. Rego M., et al., Regulation of the activation of the Fanconi anemia pathway by the p21 cyclin-dependent kinase inhibitor. Oncogene, 2012. 31(3): p. 366. https://doi.org/10.1038/onc.2011.237 PMID: 21685936

50. Garcia-Higuera I., et al., Interaction of the Fanconi anemia proteins and BRCA1 in a common pathway. Mol Cell, 2001. 7(2): p. 249–62. PMID: 11239454

51. Yamamoto K., et al., Fanconi anemia protein FANCD2 promotes immunoglobulin gene conversion and DNA repair through a mechanism related to homologous recombination. Molecular and cellular biology, 2005. 25(1): p. 34–43. https://doi.org/10.1128/MCB.25.1.34-43.2005 PMID: 15601828

52. Kim H. and D'Andrea A.D., Regulation of DNA cross-link repair by the Fanconi anemia/BRCA pathway. Genes & development, 2012. 26(13): p. 1393–1408.

53. Xia B., et al., Control of BRCA2 cellular and clinical functions by a nuclear partner, PALB2. Molecular cell, 2006. 22(6): p. 719–729. https://doi.org/10.1016/j.molcel.2006.05.022 PMID: 16793542

54. Zhang F., et al., PALB2 functionally connects the breast cancer susceptibility proteins BRCA1 and BRCA2. Molecular Cancer Research, 2009. 7(7): p. 1110–1118. https://doi.org/10.1158/1541-7786.MCR-09-0123 PMID: 19584259

55. Sy S.M.-H., et al., PALB2 regulates recombinational repair through chromatin association and oligomerization. Journal of Biological Chemistry, 2009. 284(27): p. 18302–18310. https://doi.org/10.1074/jbc.M109.016717 PMID: 19423707

56. Sy S.M., Huen M.S., and Chen J., PALB2 is an integral component of the BRCA complex required for homologous recombination repair. Proceedings of the National Academy of Sciences, 2009. 106(17): p. 7155–7160.

57. Xia B., et al., Fanconi anemia is associated with a defect in the BRCA2 partner PALB2. Nature genetics, 2007. 39(2): p. 159. https://doi.org/10.1038/ng1942 PMID: 17200672

58. Bick G., et al., Coordination of the recruitment of the FANCD2 and PALB2 Fanconi anemia proteins by an ubiquitin signaling network. Chromosoma, 2017. 126(3): p. 417–430. https://doi.org/10.1007/s00412-016-0602-9 PMID: 27277787

59. Gillespie K.A., et al., Human papillomaviruses recruit cellular DNA repair and homologous recombination factors to viral replication centers. Journal of virology, 2012. 86(17): p. 9520–9526. https://doi.org/10.1128/JVI.00247-12 PMID: 22740399

60. Bristol M.L., Das D., and Morgan I.M., Why Human Papillomaviruses Activate the DNA Damage Response (DDR) and How Cellular and Viral Replication Persists in the Presence of DDR Signaling. Viruses, 2017. 9(10): p. 268.

61. Mehta K. and Laimins L., Human Papillomaviruses Preferentially Recruit DNA Repair Factors to Viral Genomes for Rapid Repair and Amplification. mBio, 2018. 9(1): p. e00064–18. https://doi.org/10.1128/mBio.00064-18 PMID: 29440569

62. Gagnon D., Lehoux M., and Archambault J., Artificial Recruitment of UAF1-USP Complexes by a PHLPP1-E1 Chimeric Helicase Enhances Human Papillomavirus DNA Replication. J Virol, 2015. 89(12): p. 6227–39. https://doi.org/10.1128/JVI.00560-15 PMID: 25833051

63. Ishiai M., et al., FANCI phosphorylation functions as a molecular switch to turn on the Fanconi anemia pathway. Nat Struct Mol Biol, 2008. 15(11): p. 1138–46. https://doi.org/10.1038/nsmb.1504 PMID: 18931676

64. Zhang J., et al., Altered expression of FANCL confers mitomycin C sensitivity in Calu-6 lung cancer cells. Cancer Biol Ther, 2006. 5(12): p. 1632–6. PMID: 17106252

65. Shen Y., et al., Mutated Fanconi anemia pathway in non-Fanconi anemia cancers. Oncotarget, 2015. 6(24): p. 20396. https://doi.org/10.18632/oncotarget.4056 PMID: 26015400

66. Taniguchi T., et al., Disruption of the Fanconi anemia-BRCA pathway in cisplatin-sensitive ovarian tumors. Nat Med, 2003. 9(5): p. 568–74. https://doi.org/10.1038/nm852 PMID: 12692539

67. Huang Y. and Li L., DNA crosslinking damage and cancer—a tale of friend and foe. Transl Cancer Res, 2013. 2(3): p. 144–154. https://doi.org/10.3978/j.issn.2218-676X.2013.03.01 PMID: 23998004

68. Shukla P., et al., DNA interstrand cross-link repair: understanding role of Fanconi anemia pathway and therapeutic implications. Eur J Haematol, 2013.

69. Rosenberg P.S., Greene M.H., and Alter B.P., Cancer incidence in persons with Fanconi anemia. Blood, 2003. 101(3): p. 822–826. https://doi.org/10.1182/blood-2002-05-1498 PMID: 12393424

70. Nakanishi K., et al., Homologous recombination assay for interstrand cross-link repair. Methods Mol Biol, 2011. 745: p. 283–91. https://doi.org/10.1007/978-1-61779-129-1_16 PMID: 21660700

71. Kim J.M., et al., Cell cycle-dependent chromatin loading of the Fanconi anemia core complex by FANCM/FAAP24. Blood, 2008. 111(10): p. 5215–22. https://doi.org/10.1182/blood-2007-09-113092 PMID: 18174376

72. Wang Y., et al., MicroRNA-138 modulates DNA damage response by repressing histone H2AX expression. Mol Cancer Res, 2011. 9(8): p. 1100–11. https://doi.org/10.1158/1541-7786.MCR-11-0007 PMID: 21693595

73. Gyori B.M., et al., OpenComet: an automated tool for comet assay image analysis. Redox biology, 2014. 2: p. 457–465. https://doi.org/10.1016/j.redox.2013.12.020 PMID: 24624335

74. Teh M.-T., et al., Upregulation of FOXM1 induces genomic instability in human epidermal keratinocytes. Molecular cancer, 2010. 9(1): p. 45.